

# Hydroclimate volatility on a warming Earth

Daniel L. Swain<sup>1,2,3</sup>✉, Andreas F. Prein<sup>3,4</sup>, John T. Abatzoglou<sup>5</sup>, Christine M. Albano<sup>6</sup>, Manuela Brunner<sup>7,8,9</sup>, Noah S. Diffenbaugh<sup>10</sup>, Deepti Singh<sup>11</sup>, Christopher B. Skinner<sup>12</sup> & Danielle Touma<sup>13</sup>

## Abstract

Hydroclimate volatility refers to sudden, large and/or frequent transitions between very dry and very wet conditions. In this Review, we examine how hydroclimate volatility is anticipated to evolve with anthropogenic warming. Using a metric of ‘hydroclimate whiplash’ based on the Standardized Precipitation Evapotranspiration Index, global-averaged subseasonal (3-month) and interannual (12-month) whiplash have increased by 31–66% and 8–31%, respectively, since the mid-twentieth century. Further increases are anticipated with ongoing warming, including subseasonal increases of 113% and interannual increases of 52% over land areas with 3 °C of warming; these changes are largest at high latitudes and from northern Africa eastward into South Asia. Extensive evidence links these increases primarily to thermodynamics, namely the rising water-vapour-holding capacity and potential evaporative demand of the atmosphere. Increases in hydroclimate volatility will amplify hazards associated with rapid swings between wet and dry states (including flash floods, wildfires, landslides and disease outbreaks), and could accelerate a water management shift towards co-management of drought and flood risks. A clearer understanding of plausible future trajectories of hydroclimate volatility requires expanded focus on the response of atmospheric circulation to regional and global forcings, as well as land–ocean–atmosphere feedbacks, using large ensemble climate model simulations, storm-resolving high-resolution models and emerging machine learning methods.

## Sections

Introduction

Changes in hydroclimate volatility

Mechanisms underpinning hydroclimate volatility

Cascading societal and ecological impacts of hydroclimate volatility

Summary and future perspectives

A full list of affiliations appears at the end of the paper. ✉e-mail: [dlswain@ucanr.edu](mailto:dlswain@ucanr.edu)

## Introduction

Hydroclimatic variability manifests as fluctuations between unusually dry or wet meteorological conditions on timescales of days to decades. One component of this variability is hydroclimate volatility – a collective term describing anomalously frequent, sudden and/or high-magnitude transitions from wet-to-dry conditions or dry-to-wet conditions relative to a local baseline. From a water balance perspective, such extremes can be viewed as involving alternation between ‘supply surplus’ (that is, heavy precipitation causing an overabundance of water) and ‘supply deficit’ and/or ‘excess demand’ (that is, low precipitation and/or high evapotranspiration causing a deficit of water)<sup>1</sup>. Thus, hydroclimate volatility encompasses phenomena previously described using a wide range of language and terminology, including hydroclimatic intensity<sup>2,3</sup> or variability<sup>4</sup>, hydrological intensity<sup>1,5</sup>, event-to-event variation<sup>6</sup>, transitions between wet and dry periods<sup>7</sup>, drought–pluvial seesaws<sup>8</sup>, drought and pluvial transitions<sup>9</sup>, consecutive dry and wet extremes<sup>10</sup>, compound whiplash events<sup>11</sup>, accelerated swings between dry and wet spells<sup>12</sup>, precipitation whiplash<sup>13–15</sup>, precipitation variability<sup>16–19</sup>, and weather<sup>20</sup> or climate<sup>21</sup> whiplash.

Many such rapid dry-to-wet and wet-to-dry transitions have occurred across the globe – often posing formidable threats to human health and public safety, food and water security, and infrastructure (Fig. 1 and Supplementary Information). The impacts of such hydroclimate volatility are often more severe than those associated with drought or flood events in isolation; the compounding effects of transitions can increase the physical magnitude of resulting shocks as well as the odds that adaptive responses are overwhelmed by the rapid succession of opposing hydroclimate extremes across a wide range of geographies. During the winter of 2022–2023, for example, a prolonged sequence of heavy precipitation events following several years of severe drought and wildfires in California led to extensive infrastructure and property damage from widespread flooding and hundreds of shallow landslides, culminating in disaster declarations in 40 of the state’s 58 counties; in a single 3-week period, nine consecutive atmospheric river storms dropped record-breaking precipitation, and; seasonal accumulations were ultimately the greatest on record in central portions of the state. In East Africa, torrential rains during the 2023 autumn harvest season followed five consecutive seasons of drought between 2020 and 2023 (which itself brought food insecurity to over 20 million people), destroying thousands of hectares of crops and displacing more than 2 million people from their homes.

Hydroclimate volatility is also anticipated to increase beyond historical baselines in a warming climate. This increase stems, in part, from the longstanding expectation that underlying precipitation and evaporation extremes will themselves intensify owing to the fundamental thermodynamics of a warming atmosphere<sup>22,23</sup>. Existing projections of potential future hydroclimate volatility are stark: in a moderate emission scenario, hydrologically intense years are projected to triple in major global river basins<sup>5</sup>; in a high warming scenario, extreme dry-to-wet transitions could quintuple over global land areas<sup>8</sup>. Given the considerable socio-environmental impacts of such rapid transitions, better characterization of any changes – in particular, differentiating higher-confidence trends at global scales from lower-confidence trends at regional scales (including the identification of locations where volatility hotspots overlap with high societal vulnerability) – is necessary to inform effective and equitable adaptation options in the longer term. Meanwhile, improved understanding of the underlying atmospheric processes would further enhance prediction of acute episodes, allowing for more proactive emergency planning and response.

In this Review, we bring together knowledge of hydroclimate volatility in the context of anthropogenic climate change. We first assess observed and projected changes in hydroclimate volatility. Next, we explore the underlying physical causes of these changes, before outlining their observed and theorized societal and ecological effects. Finally, we discuss outstanding questions and persistent uncertainties, offering potential solutions.

## Changes in hydroclimate volatility

The characterization and quantification of observed and projected changes in hydroclimate volatility are influenced by the existence of various definitions and metrics. A holistic definition and quantitative metric of hydroclimate volatility is now offered, before synthesizing evidence of observed and projected trends.

## Defining hydroclimate volatility

The quantification of hydroclimate volatility is challenged by the inherent asymmetry in the spatiotemporal characteristics and underlying drivers of constituent wet and dry events<sup>24</sup>. Extreme precipitation can occur on timescales as short as minutes to hours and spatial scales as localized as a single neighbourhood in a large city<sup>25</sup>. In contrast, droughts typically unfold on timescales ranging from weeks to years<sup>26</sup> and can affect vast regions up to the scale of continents<sup>27,28</sup>. Moreover, whereas extreme wet events are essentially always caused by heavy precipitation, extreme dry events are generally caused by a combination of anomalously low precipitation and high evapotranspiration<sup>29</sup>, the relative importance of which can vary greatly between regions and events<sup>30–32</sup>.

This marked contrast between localized, short-duration wet extremes and spatially extensive, slowly evolving dry extremes complicates efforts to produce a single quantitative metric capturing both ends of the hydroclimate spectrum. As a result, a wide range of language and definitions has emerged to characterize changes in hydroclimate volatility. Most common are precipitation-only (‘supply side’) definitions, in which the role of evaporation or atmospheric evaporative demand is not evaluated (for example, those involving precipitation variability, intensity and/or duration of precipitation-free intervals)<sup>2,33</sup>. However, definitions incorporating evapotranspiration-related (‘demand side’) variables are increasingly favoured (for example, those involving potential evaporation, evaporative demand and/or vapour pressure deficit (VPD))<sup>1,5,24,30,34,35</sup>. Given observed non-stationarity of the climate system, there has been discussion regarding whether a universal definition of certain key hydroclimate variables is possible, or even desirable<sup>12,32,36–38</sup>.

In an attempt to overcome these challenges, here, a formal ‘hydroclimate whiplash’ metric is introduced (Supplementary Information). This metric identifies large and rapid transitions in the Standardized Precipitation Evapotranspiration Index (SPEI)<sup>29</sup>, encompassing phenomena on the supply (precipitation) and demand (evapotranspiration) sides of the distribution. Whiplash events are identified as those in which the temporal difference in monthly derived SPEI meets or exceeds the value associated with an approximate 10-year recurrence interval in the baseline data. The underlying SPEI is calculated on sub-seasonal (up to 3 months) and interannual (up to 12 months) timescales at the grid box level and relative to the underlying seasonal cycle during the historical SPEI calibration period, thus accounting for the local background degree of hydroclimate variability and seasonality. The total number of hydroclimate whiplash events is calculated as the combined sum of wet-to-dry and dry-to-wet events. Observed whiplash is

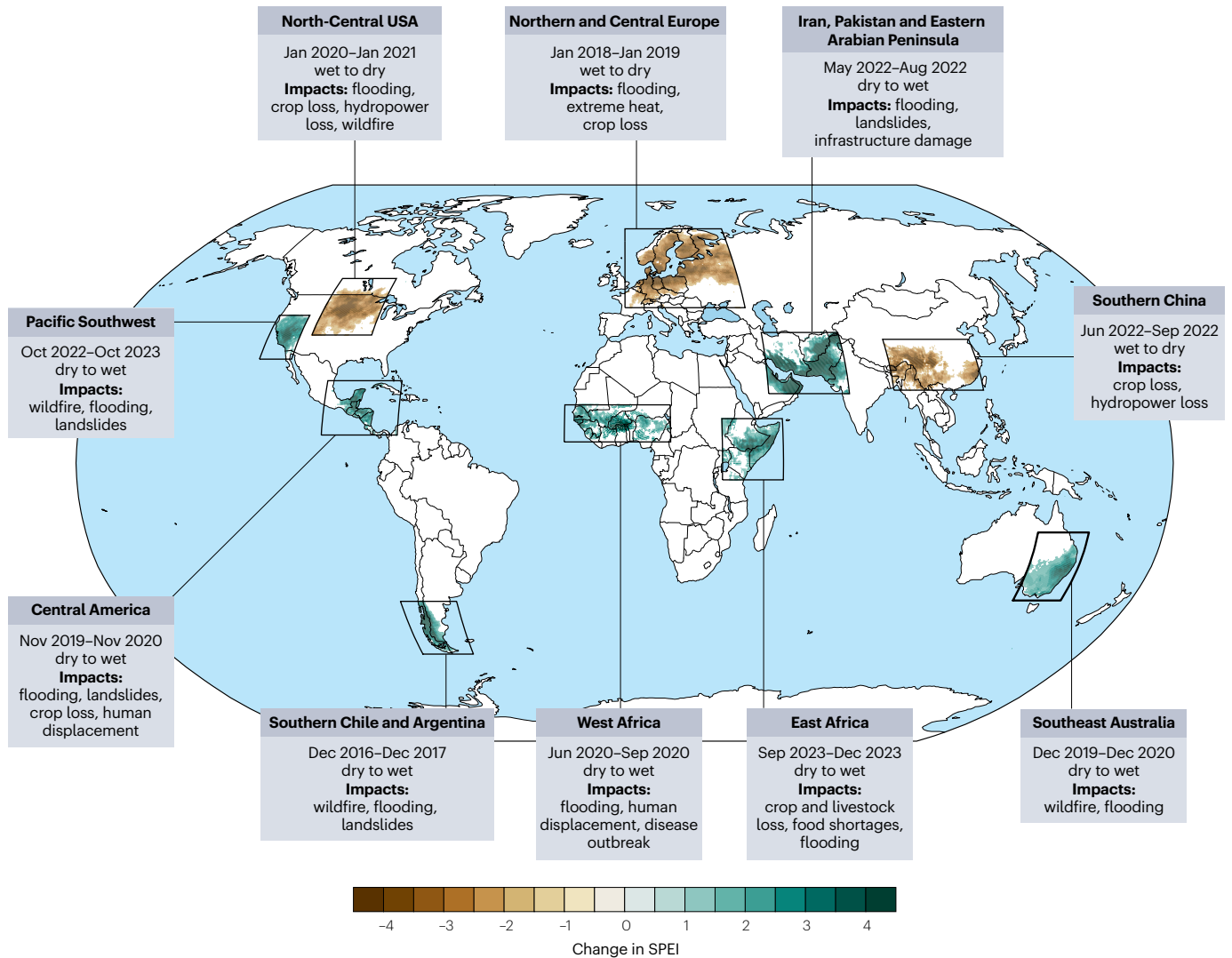


**Fig. 1 | Global hydroclimate whiplash events.** Location, date and impacts of select hydroclimate whiplash events from 2016 to 2023, and the corresponding magnitude of changes in the Standardized Precipitation Evapotranspiration Index (SPEI; shading). The brown shades represent wet-to-dry events and green shades dry-to-wet events. The events do not represent a comprehensive

catalogue of all whiplash events but are illustrative of the breadth and diversity of geographies subject to such rapid transitions. Societally and ecologically consequential hydroclimate whiplash events can occur in virtually all land areas globally, and their impacts can be strongly affected by the direction of change (from wet to dry or dry to wet).

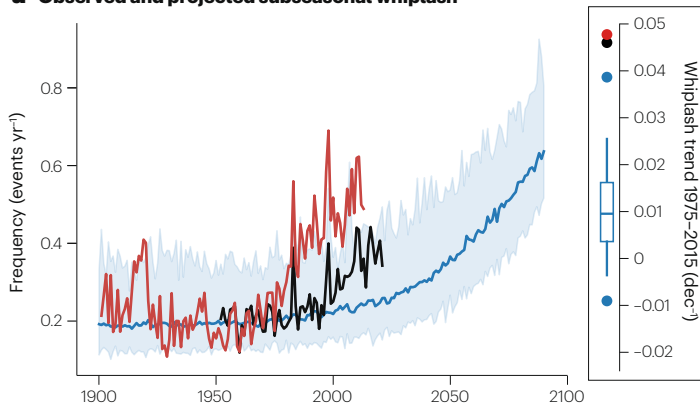
calculated using ERA5 atmospheric reanalysis<sup>39</sup> and the NOAA-CIRES-DOE 20CrV3 reanalysis (hereafter NCD20C)<sup>40</sup>, and projected whiplash is calculated using the Community Earth System Model Version 2 Large Ensemble Experiment (CESM2-LE)<sup>41</sup>.

### Trends in historical hydroclimate volatility

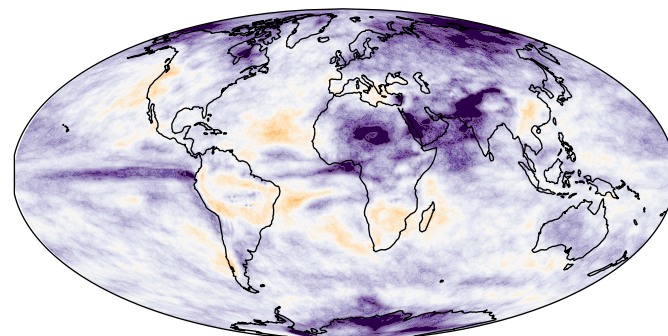
There is substantial and growing evidence that global hydroclimate volatility, defined and quantified in multiple ways, increased over the historical period. These increases are also evident when considering hydroclimate whiplash as specifically defined here (Fig. 2 and Supplementary Fig. 1). For example, over 1975–2015, the global subseasonal hydroclimate whiplash frequency increased by 31% (0.05 events per year per decade), 66.4% (0.06 events per year per decade) and 11% (0.01 events per year per decade) for ERA5, NCD20C and CESM2, respectively

(Fig. 2a). Whiplash changes over land area are slightly smaller, totalling 16.5%, 49.4% and 17.2% for ERA5, NCD20C and CESM2, respectively. Likewise, global interannual whiplash increased by 7.6% (0.02 events per year per decade), 31.3% (0.03 events per year per decade) and 3.8% (0.003 events per year per decade) for ERA5, NCD20C and CESM2, respectively (Fig. 2c), and the changes over land area were –3%, +21.9% and +7.6%. The magnitude of historical changes thus exhibits marked dataset dependency, with indications that observed changes might be outpacing model-based expectations (Fig. 2a,c). Indeed, observed trends are stronger than simulated median trends for both subseasonal (Fig. 2a) and interannual (Fig. 2c) whiplash, with the magnitude of globally averaged observed subseasonal trends (+0.05 events per year per decade) falling above the CESM2-LE ensemble spread of simulated trends (–0.01 to +0.038 events per year per decade) in ERA5 and NCD20C (Fig. 2a).

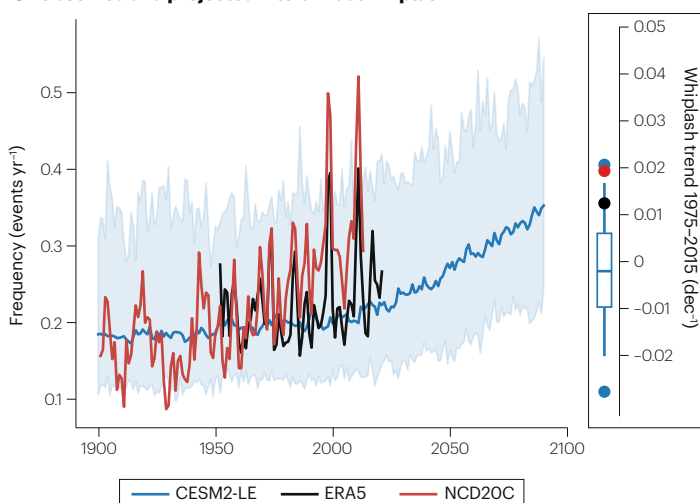
## a Observed and projected subseasonal whiplash



## b Historical subseasonal whiplash trend



## c Observed and projected interannual whiplash



## d Historical interannual whiplash trend

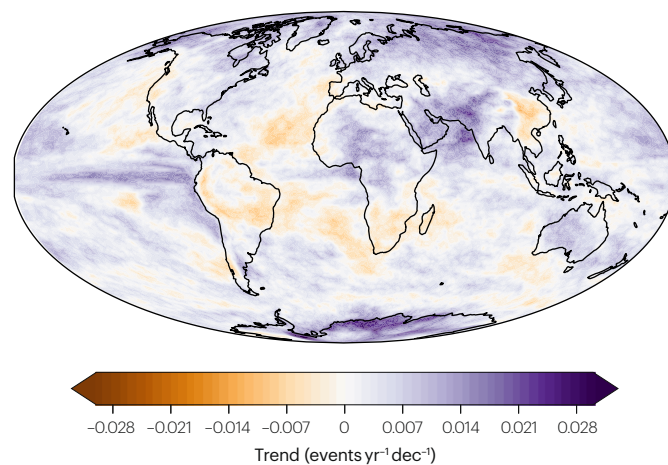


**Fig. 2 | Historical hydroclimate whiplash frequency trends. a,** A time series of global weighted-average historical subseasonal hydroclimate whiplash (3-month Standardized Precipitation Evapotranspiration Index (SPEI) with large transitions within a 3-month period) frequency in the CESM2-LE<sup>41</sup> (blue), ERA5 (ref. 39) (black) and NCD20C<sup>40</sup> (red) reanalyses. The CESM2-LE time series reflects ‘historical’ anthropogenic plus natural forcings to 2014 and SSP 3-7.0 forcing thereafter, with the solid blue line representing the median and the shading the full ensemble spread. The box-and-whisker plots to the right depict the distribution of decadal whiplash trends of each ensemble member in CESM2-LE from 1975 to 2015 and the corresponding trends for ERA5 and NCD20C. The box depicts the interquartile spread, the whiskers the 5th to 95th percentile spread and the blue circles the maximum and minimum trends. Dec, decade. **b,** Linear trends in subseasonal hydroclimate whiplash frequency over 1940–2023 in CESM2-LE. **c,** As in **a**, but for interannual whiplash (12-month SPEI with substantial transitions within a 12-month period). **d,** As in **b**, but for interannual whiplash. Climate model ensemble simulations and atmospheric reanalysis suggest that global hydroclimate whiplash probably increased between 1940 and 2023, particularly for subseasonal whiplash, but with substantial spatial heterogeneity.

from 1975 to 2015 and the corresponding trends for ERA5 and NCD20C. The box depicts the interquartile spread, the whiskers the 5th to 95th percentile spread and the blue circles the maximum and minimum trends. Dec, decade. **b,** Linear trends in subseasonal hydroclimate whiplash frequency over 1940–2023 in CESM2-LE. **c,** As in **a**, but for interannual whiplash (12-month SPEI with substantial transitions within a 12-month period). **d,** As in **b**, but for interannual whiplash. Climate model ensemble simulations and atmospheric reanalysis suggest that global hydroclimate whiplash probably increased between 1940 and 2023, particularly for subseasonal whiplash, but with substantial spatial heterogeneity.

Although it is clear that the overall global frequency of hydroclimate whiplash events has increased, there remains considerable uncertainty regarding the spatial pattern and magnitude of these changes. The spatial patterns vary markedly between reanalysis datasets and model simulations (Supplementary Fig. 1). A substantial portion of this apparent mismatch can probably be attributed to the degree to which each dataset captures the underlining anthropogenic forcing: ERA5 and NCD20C each represent a single representation of all plausible sequences of historical whiplash events (incorporating substantial statistical noise from internal variability in addition to the anthropogenic warming signal), whereas CESM2-LE represents the ensemble average across 100 members, smoothing out simulated internal variability and potentially yielding a more reliable estimate of the forced

response<sup>42</sup>. Meanwhile, genuine observational uncertainties and differences in data assimilation schemes probably explain differences between ERA5 and NCD20C. For these reasons, CESM2-LE projections (Fig. 2b,d) might offer a more statistically robust depiction of spatial patterns expected from historical forcings. Projected whiplash trends are generally greater in magnitude for subseasonal (Fig. 2b) than for interannual (Fig. 2c) whiplash, although the spatial pattern is similar and is characterized by strong increases across most of northern Africa, the Middle East, South Asia, northern Eurasia, the tropical Pacific and the tropical Atlantic; modest decreases are apparently across the subtropical North and South Atlantic, northern South America, southern Africa, portions of southeastern Asia and a portion of the subtropical North Pacific.



These findings of enhanced hydroclimate whiplash are consistent with broader evidence of rising hydroclimate volatility from various datasets, time periods and metrics. On the supply side, daily precipitation variability increased at most observation sites<sup>16</sup>, with the trend accelerating over time and being most prominent in Europe, Australia and eastern North America<sup>43</sup>, while global average daily precipitation variability increased by 14% between 1900 and 2020 (ref. 43). Subseasonal precipitation-based metrics additionally indicate increases in observed global land-only hydroclimate volatility between 1979 and 2019, consistent with a projected time of emergence – that is, the time at which anthropogenic signals emerge above background natural variability – estimated at ~2017 over land<sup>15</sup> by climate model large ensembles. Further evidence of changing historical volatility at regional to continental scales comes from integrated measures of precipitation intensity and dry spell length<sup>2</sup>, and also locally from tree-ring-based palaeoclimate reconstructions of precipitation, streamflow and snow water in California, which suggest that twentieth-century increases in variability are probably unprecedented in a multi-centennial (~600 year) context<sup>4</sup>.

Combined supply and demand metrics, as well as those directly examining compound hydroclimatic transitions, also reveal rising volatility. For example, the surplus deficit intensity index (an aggregate measure of variation in atmospheric water supply and demand) suggests that global terrestrial hydrological intensity increased by approximately half a standard deviation unit between 1979 and 2017 (ref. 1). Likewise, analysis of the Palmer Drought Severity Index demonstrates increasing geographically remote but temporally coincident wet and dry extremes between 1950 and 2014 (ref. 24), and analysis of terrestrial water storage anomalies using observations from gravity-monitoring satellites reveals widespread intensity increases between 2002 and 2021 (ref. 44). The frequency and/or intensity of transitions between wet and dry conditions have also risen over the historical period. For instance, a soil-moisture-based metric demonstrates robust global increases in rapid drought and pluvial transitions between 1980 and 2022 (ref. 9), coincident with rising intraseasonal compound wet to warm and dry events in Asia over 1979–2014 (ref. 11).

## Trends in projected hydroclimate volatility

Consistent with theoretical expectations<sup>45</sup>, there is strong consensus that historical increases in hydroclimate volatility will continue with ongoing anthropogenic warming. These changes are projected to be larger over land areas compared with the ocean, with their magnitude exhibiting strong dependency on the degree of anthropogenic warming (Fig. 3). For example, over land areas, globally averaged subseasonal hydroclimate whiplash frequency increases 19% (from 0.1 to 0.12 events per year), 113% (from 0.1 to 0.2 events per year) and 266% (from 0.1 to 0.4 events per year) for 1 °C, 3 °C and 5 °C warming, respectively, relative to the 1940–1980 reference (Fig. 3a). The magnitude of subseasonal whiplash increases is smaller over ocean areas, reaching 9.3% (from 0.2 to 0.22 events per year), 62.7% (from 0.2 to 0.33 events per year) and 143% (from 0.2 to 0.49 events per year) at 1 °C, 3 °C and 5 °C warming, respectively (Fig. 3a). Spatially, these subseasonal whiplash increases are nearly ubiquitous over the globe by ~3 °C of warming (Fig. 3b); modest negative trends (generally ≤25%) are projected only for portions of land areas in southern Africa and central Chile, as well as slightly larger decreases over subtropical portions of the Atlantic and Pacific oceans. These increases are generally largest in absolute terms, representing a frequency increase of 150% or more at high latitudes (especially northern Eurasia and Canada) and the deep tropical Pacific and Atlantic

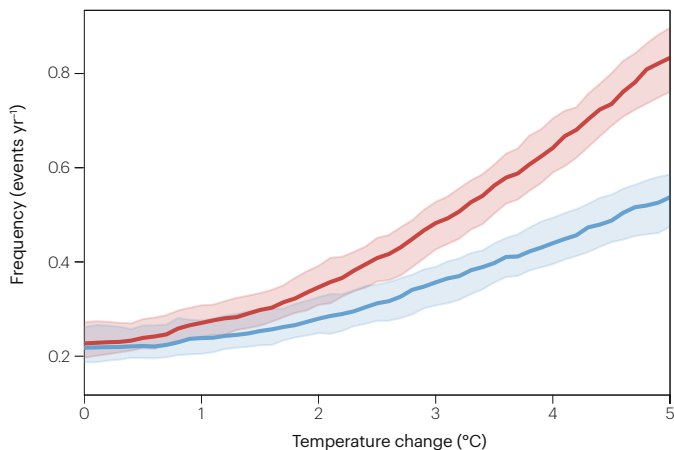
ocean basins near the Intertropical Convergence Zone, with additional regional maxima over land in a broad swath extending from northern Africa across the Arabian Peninsula into South Asia and the adjacent Tibetan Plateau<sup>14,15</sup> (Fig. 3b).

Interannual hydroclimate whiplash generally exhibits similar changes to subseasonal, but with a lower magnitude<sup>18</sup>. Indeed, interannual increases over land are 12% (from 0.1 to 0.11 events per year) at 1 °C warming, 52% (from 0.1 to 0.15 events per year) at 3 °C warming and 91% (from 0.1 to 0.2 events per year) at 5 °C warming (Fig. 3c). Increases over ocean areas are lower still at 7%, 34% and 57% at 1 °C, 3 °C and 5 °C warming, respectively (Fig. 3c). The spatial pattern of these changes largely mimics those of subseasonal whiplash (Fig. 3d), although with less pronounced and more evenly distributed maxima (increases of 50–100%) broadly across the tropics, Arctic, north Africa and South Asia. However, the area of negative trends for interannual whiplash is broader, covering a larger portion of the subtropical North and South Atlantic, South Pacific and southern Africa, and expanding to encompass a portion of the subtropical North Pacific. For both interannual and subseasonal whiplash, the contribution of precipitation changes alone is similar across oceanic and continental regions (Supplementary Fig. 2), but potential evapotranspiration amplifies increases over continents, particularly at high latitudes and across North Africa and the Middle East (Supplementary Fig. 3). These increases are not detected in precipitation-only metrics<sup>15,18,46</sup>.

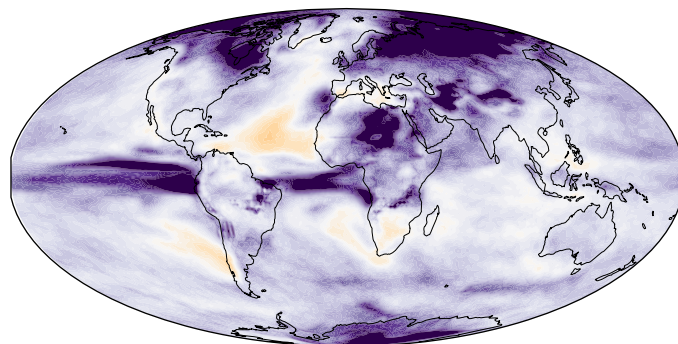
These projections are consistent with abundant evidence documenting broader volatility with warming, as represented using various hydroclimate intensity or whiplash (or whiplash-like) measures. Multiple metrics and climate model ensembles indicate hydroclimate intensification<sup>1,3</sup> and increasing precipitation variability<sup>16–18</sup> over the twenty-first century. Indeed, precipitation variability is expected to increase by 3–4% per °C globally and 4–5% per °C over land<sup>16</sup>, with the magnitude of contributions from multi-day timescales thought to be larger than that from multi-annual timescales<sup>17,18</sup>. Projected increases in whiplash or event-to-event variability lend further support. For example, at the regional scale, overall increases in both wet and dry years<sup>47</sup>, as well as 25–100% increases in extreme interannual cool season precipitation whiplash transitions and 35–85% increases in seasonal sharpness (the ratio of total annual precipitation falling during the peak winter wet season versus the autumn and spring shoulder seasons), are projected for California by the late twenty-first century under a high warming scenario<sup>13</sup>; these changes are in line with further estimates of a broader 25–60% increase in frequency and 30–100% increase in intensity of interannual precipitation whiplash (using a similar definition) across semi-arid hotspot regions (including the Mediterranean Basin, western Australia and southwestern USA) by the late twenty-first century<sup>14</sup>. In a more temperate climate setting, regional increases in lagged compound wet and dry spells<sup>12</sup> are projected in the northwestern USA and southwestern Canada. At the global scale, 60% of land area is projected to experience accelerated transitions between dry and wet periods under a high warming scenario<sup>7</sup>. The magnitude of these changes depends on the metric, method and warming scenario, but there are suggestions of 2.5× increases in globally averaged subseasonal precipitation whiplash<sup>15</sup> and 5× increases in interannual dry-to-wet events over global land areas compared with the historical period<sup>8</sup>. Additionally, hydrologically intense years are further projected to triple in major global river basins even under moderate warming<sup>5</sup>.

Several regions have emerged as having regional hydroclimate volatility responses that deviate substantially from the global mean. Generally, the high latitudes (Arctic and Antarctic, plus northern Eurasia)

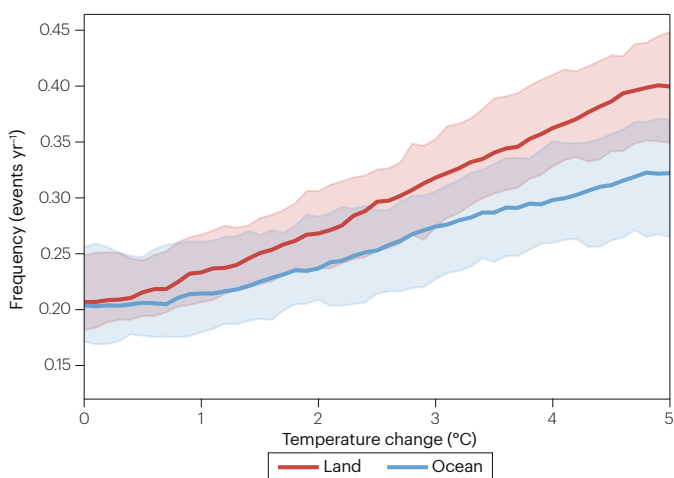
**a** Subseasonal whiplash warming sensitivity



**b** Subseasonal whiplash at 3°C warming



**c** Interannual whiplash warming sensitivity



**d** Interannual whiplash at 3°C warming

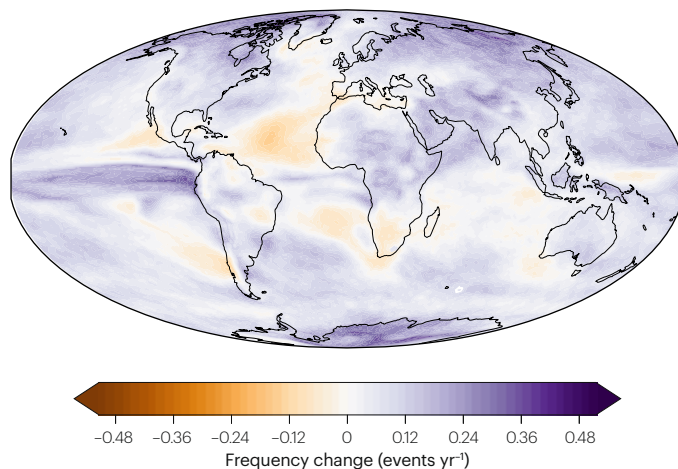


**Fig. 3 | Projected hydroclimate whiplash trends in a warming climate.**

**a**, The frequency of global weighted-average subseasonal (up to 3 months) hydroclimate whiplash events in the CESM2-LE<sup>41</sup> as a function of projected global average temperature change. The solid lines represent the median and shaded areas the 5th to 95th percentile ensemble spread. **b**, The projected trends in subseasonal hydroclimate whiplash in CESM2-LE at 3°C global mean

warming. **c**, As in **a**, but for interannual (up to 12 months) whiplash; note the different y-axis scale. **d**, As in **b**, but for interannual whiplash. All global mean temperature increases are calculated relative to the 1940–1980 reference period. Hydroclimate whiplash increases strongly with warming over nearly all global land areas and most global ocean areas outside of the subtropics.

and deep tropics (near the Intertropical Convergence Zone) over the Pacific and Atlantic basins exhibit rates greater than the global mean, whereas subtropical regions (particularly over the Pacific and Atlantic basins and small portions of adjacent land over parts of coastal Chile and southwestern Africa as well as the Mediterranean Sea) exhibit rates lower than – or even of the opposite sign from – the global mean<sup>6,7,14,15</sup> (Fig. 3a,c). When specifically considering precipitation-only volatility on interannual timescales, the largest regional increases in climatological transition zones occur just poleward of the subtropics in both hemispheres (including the southwestern USA and California<sup>13</sup>, southern and western Australia, southeastern Africa, the northern and eastern Mediterranean Basin and portions of central Europe<sup>14</sup>), resulting from locally amplified precipitation variability near boundaries separating regions of robust mean drying in the subtropics (caused primarily by storm track shifts related to the expanding Hadley cell<sup>48</sup>) and robust

mean wetting in the extratropics (caused by both storm track shifts and thermodynamic effects<sup>49,50</sup>).

Thus, hydroclimate whiplash is projected to increase in most global regions in a manner that scales with rising global mean temperature. These whiplash changes are likely to be larger in magnitude over land compared with ocean given that evaporative demand extremes can be greatly amplified via land-surface/soil-moisture feedbacks<sup>31,51,52</sup>, and also to have greater impacts given the sensitivity of human systems and the terrestrial biosphere to extremes in freshwater availability<sup>5,53</sup>.

## Mechanisms underpinning hydroclimate volatility

There is strong consensus that changes in hydroclimate volatility are fundamentally driven by thermodynamic processes at global scales. At regional scales, however, other factors become important, including

changes in atmospheric circulation (partly explaining the differences between observed and projected spatial whiplash trends; cf. Fig. 1a,b and Supplementary Fig. 1). The drivers of such volatility changes are now discussed, as are key differences between the causes of hydroclimate whiplash (defined with respect to the atmosphere) versus hydrologic whiplash (defined with respect to the land surface).

## Thermodynamics dominate, dynamics modulate

In a hydroclimate context, thermodynamic effects broadly describe the direct impacts of increased temperature upon actual and/or potential atmospheric water vapour. Fundamental thermodynamics dictate that the saturation vapour pressure of air with respect to water – and, therefore, the water-vapour-holding capacity of the atmosphere – must increase with rising temperatures, as encapsulated by the Clausius–Clapeyron (CC) equation, which predicts an exponential scaling rate of ~7% per °C (refs. 54,55). Observed increases in vertically integrated (column) atmospheric moisture content are generally in line with these expectations<sup>56</sup>, and are directly attributed to greenhouse-gas-driven warming<sup>57</sup>. This ‘thermodynamic component’<sup>58,59</sup> of climate change – that is, nonlinear increases in the water holding and water evaporating potential of the atmosphere – yields corresponding increases in extreme precipitation<sup>60</sup> and potential evapotranspiration (as reflected using the analogy of an expanding atmospheric sponge; Box 1).

While thermodynamically driven increases in extreme precipitation events have been widely recognized<sup>60</sup>, a smaller but rapidly growing body of research has focused on the drivers<sup>61–65</sup> and impacts<sup>30,46,66</sup> of increasing evaporative demand. One consequence of the exponential increase in saturation vapour pressure is a concurrent increase in the VPD – the difference between the theoretical maximum and actual

ambient absolute humidity. Importantly, VPD increases nonlinearly with temperature even under the assumption of constant relative humidity (RH), meaning that rising temperatures alone are sufficient to drive rapid increases in VPD even without changes in the fractional saturation of the air (Fig. 4). Higher VPD yields an increase in the evaporative demand of the air (that is, its potential to drive evapotranspiration from the land surface, bodies of water and living plants<sup>52,67,68</sup>) such that actual evaporation increases if water is available; if water is not available, sensible heat flux and near-surface air temperature rise.

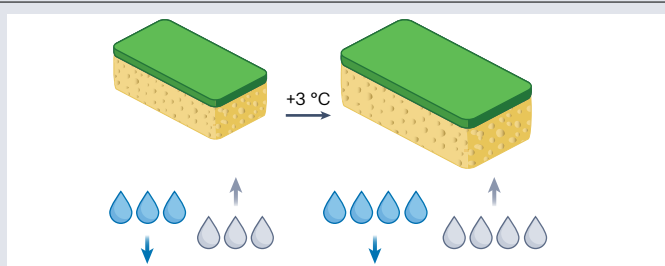
In line with these expectations, increases in mean and extreme VPD have been observed over global land areas<sup>68,69</sup> and directly attributed to anthropogenic warming<sup>64,70</sup>. Extreme VPD values are expected to increase even faster than the seasonal mean over global land areas, a nonlinearity stemming from nearly equal contributions by the underlying thermodynamics and by increased temperature and moisture variability<sup>51</sup>. These increases in mean and extreme VPD have large consequences for ecosystems<sup>68</sup>, drought<sup>35,46</sup> and wildfire<sup>70,71</sup> risks via faster and more intense soil drying<sup>31</sup> and increasingly severe and persistent aridification of vegetation<sup>72</sup>. Indeed, rates of drought intensification increased over 75% of global land regions between 1948 and 2014, with a projected future trend towards more rapidly developing flash droughts on a high warming trajectory<sup>73</sup>. This amplified VPD-related continental drying is probably a key factor explaining faster projected hydroclimate whiplash over land versus the ocean (Supplementary Fig. 3c,d), although this pattern is not yet apparent in observations (Supplementary Fig. 1), perhaps owing to increased cool El Niño–Southern Oscillation (ENSO) conditions in the late 20th and early 21st centuries<sup>74,75</sup>. The evidence that RH over a majority of global land areas will decrease<sup>62,65</sup> suggests that the already large projected increases in VPD under a constant RH assumption might well be conservative over the continents.

## Box 1 | Clausius–Clapeyron and the expanding atmospheric sponge

The saturation vapour pressure of air with respect to water – commonly referred to as the water-vapour-holding capacity of the atmosphere – increases exponentially in response to a linear increase in temperature by around 7% per °C. This thermodynamic phenomenon – the Clausius–Clapeyron (CC) relation<sup>54,55</sup> – is at the heart of the observed and projected acceleration of the global hydrologic cycle from anthropogenic warming. Indeed, one key implication is that the most extreme rates of precipitation and potential evapotranspiration will increase rapidly on a warming Earth, even in the absence of changes in RH and atmospheric circulation.

Thus, extremes on both the wet (supply) and dry (demand) side of the hydroclimate spectrum can be amplified by the very same underlying thermodynamic process.

The physical processes underpinning increasing hydroclimate volatility in a warming climate can be visualized as an expanding atmospheric sponge. Consider a series of progressively larger kitchen sponges as representing the increasing water-vapour-holding capacity of the atmosphere as temperatures rise. These hypothetical sponges become 7% larger with each degree of warming, such that at 3°C of warming, the atmospheric ‘sponge’ would be around 22.5% larger than at the pre-industrial temperature (see figure). In turn, the absorptive capacity of the sponges increases such that they can soak up more water from a damp countertop (analogous to increased



evaporation over wet surfaces), as will their propensity to yield increasingly large volumes of water if wrung out with sufficient force (analogous to increasingly heavy downpours of precipitation when atmospheric conditions are otherwise conducive).

This analogy also holds in the event that water availability is a limiting factor: just as an initially dry kitchen sponge cannot soak up any water from a dry countertop nor subsequently yield water if wrung out, an exponential increase in the equilibrium vapour pressure of the atmosphere at saturation does not itself guarantee a correspondingly large increase in overall precipitation (which is radiatively constrained in the Earth’s climate system) nor increased rates of actual evapotranspiration in water-limited environments (such as deserts).



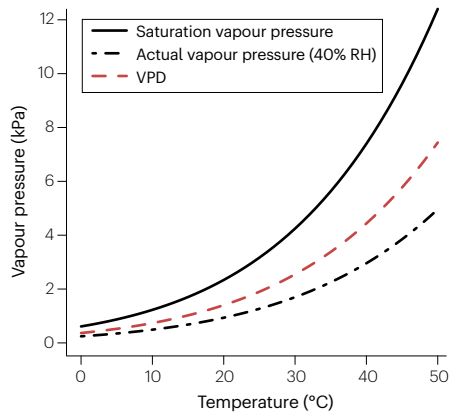


**Fig. 4 | Temperature, humidity and the VPD.** Saturation vapour pressure (solid black line), absolute humidity (dot-dashed black line; assuming 40% relative humidity (RH)) and vapour pressure deficit (VPD) (dashed red line; the difference between saturation and actual vapour pressures, assuming 40% RH) as a function of realistic Earth surface air temperatures. A nonlinear (exponential) increase in the VPD will result from a linear increase in temperature even under the assumption of constant RH.

Together, these thermodynamically driven increases in extreme precipitation and potential evapotranspiration probably explain the majority of globally averaged observed and projected changes in hydroclimate volatility through their amplification of the supply side and demand side of the global water balance, respectively<sup>1,5</sup>. Moreover, they offer a compelling potential mechanism for nonlinear increases in hydroclimate volatility with warming (Fig. 3a,c) given their close association with well-understood underlying exponential processes.

These same thermodynamic effects also underpin most regional increases in hydroclimate volatility, but changes in atmospheric circulation<sup>76</sup> (that is, dynamical effects) can substantially modify their influence locally. In general terms, dynamical changes amplify or offset large-scale thermodynamic increases in moisture by increasing or decreasing air convergence through modification of horizontal and/or vertical winds<sup>49</sup> – occasionally to a degree that dominates the net local response<sup>77</sup>. Regions where projected increases in hydroclimate volatility are greater than the global average (including the Pacific and Atlantic Ocean deep tropics, North Africa, the Arabian Peninsula, South Asia, and much of northern Eurasia and Canada) generally encompass areas where dynamical effects reinforce moisture increases (Fig. 3b,d). Regions where volatility changes are less than the global average (or are even negative in sign, most notably in the oceanic subtropics broadly and also across far southern Africa) encompass areas where dynamical effects offset or even outweigh thermodynamics (Fig. 3b,d). In tropical ocean regions and some tropical or subtropical continental regions, the volatility enhancement by dynamical changes is probably related to strengthened vertical motion (updrafts) during intense convective storms<sup>49</sup>. In subtropical regions, the volatility reduction by dynamical changes is probably related to mean drying caused by poleward-shifted mid-latitude storm tracks<sup>48</sup> (with volatility enhancement at high latitudes stemming from mean wetting via the same process).

Regional flavours of hydroclimate volatility – that is, whether changes are primarily caused by increases in extreme wet events, extreme dry events or both<sup>14</sup> – often reflect the balance of thermodynamic and dynamical changes in a particular location. Regional

hotspots of increased twenty-first century volatility include wet-dominated increases across western North America<sup>4,13,14</sup> (where dynamical changes reinforce thermodynamic changes), dry-dominated increases in the Mediterranean Basin<sup>14</sup> (where dynamical changes counteract thermodynamic changes) and mixed wet–dry increases over southern Africa<sup>14</sup> (where dynamical changes and thermodynamic changes are also mixed). When only precipitation changes are considered, most regions are anticipated to become wetter and more volatile with warming, except for subtropical regions (mainly over oceans)<sup>18</sup>. However, use of a metric that incorporates both precipitation and evaporative demand reveals a nearly universal global increase in volatility over land that is dominated by increases in extreme wet events globally and in most subregions<sup>5</sup>, although increases in extreme dry events still contribute substantially and their relative contributions rise in accordance with evaporative demand in the twenty-first century<sup>1</sup>.

Changes in the strength or spatial patterns of geographically remote teleconnection patterns – which are often proximately responsible for the onset of rapid hydroclimatic transitions<sup>46,78,79</sup> – represent another dynamical mechanism influencing future frequency and/or intensity of hydroclimate volatility. Examples include the possible increase in the occurrence of extreme ENSO events<sup>80</sup>, the projected strengthening of hydroclimatic extremes associated with the Madden–Julian Oscillation (MJO)<sup>81</sup> and the eastwards shift in associated modes of atmospheric circulation variability associated with both ENSO and MJO<sup>82,83</sup>. Although the MJO and ENSO are both inherently tropical phenomena, they are known to exert profound influences on regional to continental-scale climate<sup>84</sup>, and so changes in either their amplitude and/or the spatiotemporal characteristics of their respective teleconnections would probably have major implications for dynamical contributions (at least episodically) to changes in hydroclimate volatility; however, exactly how these changes might manifest remains subject to considerable uncertainty<sup>85</sup>.

Thus, thermodynamic effects dominate, but dynamical effects modulate observed historical and projected future increases in global hydroclimate volatility<sup>14,43,49</sup>. The comparatively high magnitude and confidence in the sign and spatial pattern of thermodynamic changes in a warming climate<sup>86</sup> overwhelms the comparatively lower magnitude (at global scales) and weaker scientific confidence (at subcontinental scales)<sup>77</sup> in dynamical changes. Indeed, observed increases in volatility over global land areas are primarily caused by a combination of atmospheric moistening and increased evaporative demand, as opposed to changes in atmospheric circulation<sup>43</sup>.

### Divergence between extreme and non-extreme precipitation

Increasing divergence between trends in extreme and non-extreme precipitation caused by anthropogenic warming is probably a further contributor to broader increases in hydroclimate volatility. Globally widespread increases in extreme precipitation events have occurred in response to anthropogenic warming<sup>87,88</sup>, and both observations and projections indicate substantial acceleration in the magnitude and relative frequency of such events as a function of event magnitude<sup>16,23,89–91</sup>. In other words, the most intense precipitation events are likely to increase faster than more moderate events on a warming Earth, resulting in broadening of the upper tails of associated statistical distributions (increased positive skewness and/or kurtosis)<sup>91,92</sup>.

Several terms have been coined to qualitatively describe the amplified intensification of precipitation in the upper tail of its distribution. These include the ‘wet regions get wetter and dry regions drier’<sup>88</sup> or ‘rich-get-richer’<sup>93</sup> hypothesis, with suggestions that such a



generalization might be more accurate in temporal rather than spatial terms<sup>94</sup>; the ‘higher intensity, reduced frequency’ response of precipitation to warming, highlighting the general tendency for light to moderate precipitation to decrease in frequency but for heavy precipitation to increase<sup>3</sup>; and the ‘wet get more variable’ paradigm, suggesting that the propensity for increased precipitation volatility is greater in climatologically wet versus dry regions<sup>18</sup>.

This nonlinearity in the response of precipitation extremes can be attributed to multiple physical processes. Although thermodynamic increases in atmospheric water vapour saturation capacity of  $-7\%$  per  $^{\circ}\text{C}$  (ref. 95) are associated with an increase in extreme precipitation of similar magnitude when averaged over space, time and precipitation intensities<sup>96,97</sup>, global mean precipitation increases at a rate of only  $-2-3\%$  per  $^{\circ}\text{C}$  owing to constraints set by the global atmospheric energy budget<sup>98</sup>. Such divergence leads to a compensating decrease in non-extreme precipitation that is nearly ubiquitous at all latitudes<sup>94</sup>, as confirmed in model simulations<sup>3</sup> and observations<sup>23,99</sup>. In particular, there is a broad decrease in the frequency and intensity of light-to-moderate precipitation, an increase in the overall number of dry days ( $>30$  days per year over the Mediterranean and Amazon regions on a high warming trajectory, but no increase in polar regions<sup>100</sup>) and an increase in dry spell length in some regions, especially in the tropics and subtropics during the dry season<sup>101</sup>. Increases in the most intense precipitation events, which can themselves be partially self-amplifying via convective feedbacks in a warming climate<sup>102,103</sup>, might further accentuate this compensatory effect by subsequently stabilizing the atmospheric column through latent heat release<sup>22</sup> and decreasing lighter precipitation events.

One consequence of this higher intensity, reduced frequency response<sup>3</sup> is that the relative and absolute increase in precipitation extremes increases as a function of event intensity. Lesser extremes (95th percentile daily precipitation) increase at a rate slower ( $3\%$  per  $^{\circ}\text{C}$ ) than growth in atmospheric water vapour ( $7\%$  per  $^{\circ}\text{C}$ ), but rarer and higher magnitude extremes (99.9th percentile daily precipitation) increase at a rate near or even exceeding growth in water vapour ( $>7\%$  per  $^{\circ}\text{C}$ )<sup>104</sup>. Indeed, the most extreme precipitation events might be associated with super-CC increases in intensity, substantially exceeding  $7\%$  per  $^{\circ}\text{C}$  (ref. 103), especially when associated with shorter-duration (hourly to subhourly) convective extremes<sup>103,105</sup> or the inner core of tropical cyclones<sup>106</sup>. Although there is not universal agreement on super-CC increases in all settings<sup>107</sup>, precipitation scaling as high as  $14\%$  per  $^{\circ}\text{C}$  has been found in the tropics<sup>96</sup> and the very highest magnitude events elsewhere<sup>102</sup>. The processes causing these super-CC increases vary according to the underlying precipitation-generating mode and storm characteristics, but increased moisture convergence stemming from regional shifts in atmospheric circulation<sup>89</sup> or nonlinear effects related to the vertical profile of latent heat release by precipitation in clouds<sup>103</sup> might be a major contributor.

## Hydroclimate versus hydrological volatility

Although the meteorological drivers of hydroclimate volatility are relatively well understood, the terrestrial drivers of hydrological volatility – which describes rapid transitions between dry and wet states of the land surface – can be distinct from their atmospheric counterparts. Whether hydroclimate volatility yields hydrological volatility depends on various factors such as underlying geography, geology, land use and antecedent hydrological conditions (including soil moisture, snow cover and groundwater)<sup>108,109</sup>. Therefore, land-surface processes can either weaken or intensify hydroclimatic whiplash events (for example,

if soils are particularly dry or wet before an extreme precipitation event, reducing or amplifying flood risk, respectively), or even lead to hydrological volatility in the absence of hydroclimatic whiplash (for example, non-extreme precipitation co-occurring with heavy snowmelt, amplifying flood risk)<sup>110</sup>.

Less is known about the mechanisms of hydrological volatility compared with hydroclimate volatility. Climate change is already thought to be influencing antecedent soil moisture conditions relevant to hydrologic whiplash episodes, including the widespread global drying of root zone soil moisture<sup>111</sup>. Broad drying of shallow soil moisture might be expected to reduce the risk of smaller floods in a warming climate owing to increased soil water absorptive capacity. However, the risk of extreme floods is not expected to be reduced, and might increase because increasingly extreme precipitation events eventually overwhelm the mitigating influence of drier soils. This divergence can be viewed as a form of flood extremeness whiplash<sup>109,112,113</sup> (Box 2). In specific regions where seasonal and/or regional trends are towards wetter antecedent conditions, flood magnitudes will increase at an even faster rate than precipitation extremes owing to the synergistic effect of saturated antecedent soil conditions and faster and/or earlier snowmelt<sup>110,114</sup>. Opposing changes at opposite ends of this spectrum emerge in hydrological projections for California, for instance – where anthropogenic warming results in changes of opposite sign in the upper and lower tails of the run-off distribution despite little change in mean streamflow – owing to increases in winter run-off that occur despite run-off declines in all other seasons<sup>92</sup>.

## Cascading societal and ecological impacts of hydroclimate volatility

Given the observed historical impacts of hydroclimate whiplash events, and the strong consensus that they will increase in frequency and amplitude in a warming climate and that societal and ecological responses to increasingly wide swings between extreme dry and wet conditions are probably nonlinear, there is an urgent need to understand and plan for such volatility changes. The impacts of hydroclimate volatility and possible adaptation options are now discussed.

## Consequences for natural and human systems

Increases in hydroclimate volatility have the potential to impact various socio-environmental systems. For instance, rapid transitions between extreme wet and extreme dry can impact water quality via harmful algal blooms<sup>115</sup> (when hot and dry conditions follow a burst of nutrient-rich run-off into a reservoir during heavy rains)<sup>116</sup> or the influx of excess organic and/or mineral content (when heavy rains following severe drought and/or elevated wildfire activity wash silt, ash or woody debris into bodies of water)<sup>117</sup>. This degradation has resulting influences on freshwater ecosystems and water security. Hydroclimate volatility also has a bearing on food security through decreased plant productivity<sup>118,119</sup>, crop failures<sup>120</sup>, damage to agricultural land or displacement of agricultural workers<sup>121</sup>, livestock mortality or decreased grazing viability<sup>122</sup>, access disruptions<sup>123</sup> and pest outbreaks<sup>124</sup>. Rapid hydrological shifts further present a public health threat when hydroclimate volatility brings about population surges in potential disease vectors such as rodents or mosquitoes<sup>125</sup>, or increases in pathogen-specific overlap of favourable temperature and moisture conditions<sup>126</sup>; when water sources become overly concentrated and/or contaminated during very low or very high run-off conditions (elevating the risk of water borne diseases<sup>127</sup>); or when the life cycle of soil-borne fungal pathogens depends on the alternation between wet soils for

## Box 2 | Resolving the extreme precipitation–flood paradox

There is a strong expectation that precipitation extremes will increase with anthropogenic warming<sup>60,189,190</sup>, and compelling evidence that they have already done so<sup>88,191–193</sup>. Yet the evidence base for systematic increases in flooding is weaker<sup>194,195</sup>, with suggestions that the overall frequency of floods has decreased regionally<sup>196,197</sup>, although with considerable spatial variation<sup>195</sup>. This counterintuitive observation describes the extreme precipitation–flood paradox<sup>198</sup>.

To explain this paradox, flood responses to warming have been examined along a spectrum of intensity — essentially asking whether very large (and therefore rarely observed<sup>199</sup>) floods might change differently from smaller, more commonly observed events. In doing so, a more nuanced picture emerges: whereas smaller and more frequently observed floods exhibit geographically mixed increasing and decreasing trends<sup>195</sup>, initial indications suggest that the most extreme and rarely observed floods might be increasing<sup>200</sup>, although with substantial uncertainty given the presence of confounding factors that vary geographically and by climate zone<sup>194,195</sup>. Targeted analyses that span the full spectrum of flood intensity<sup>113</sup> or focused specifically on large, rarer floods<sup>200</sup>, or that leverage large ensemble

modelling experiments<sup>109</sup> and palaeoclimate data<sup>112</sup> to increase the effective sample size of flood events, have helped to demonstrate this counterintuitive effect.

This predicted and observed divergence in the direction of change in flood magnitudes across their intensity spectrum can ultimately be explained by differences in the relative importance of different flood generation processes<sup>195</sup>. Moderate floods with short recurrence intervals are strongly influenced by changes in land-surface conditions (such as soil moisture and snowmelt), whereas extreme floods with long recurrence intervals are more directly influenced by the magnitude of extreme precipitation events<sup>200,201</sup>, which tend to overwhelm the otherwise mitigating influence of soil drying in a warming climate<sup>109,201</sup>. These findings raise the prospect that increasing hydroclimate volatility will subsequently lead to increased hydrological volatility in the form of fewer small floods (which often bring ecological net benefits), but more frequent extreme floods (which tend to be the most destructive and harmful events) — an outcome termed the ‘worst of both worlds’ scenario<sup>200</sup>.

growth and later transition to dry soil conditions for aerosolization<sup>128</sup>. Geophysical effects such as landslides<sup>129</sup> and cracking of clay-rich soils from expansion and contraction might also occur, in turn potentially damaging buildings and water and transportation infrastructure<sup>130,131</sup>.

Hydroclimate volatility can also yield geophysical and societal effects that are distinct from and/or greater in magnitude than those associated with isolated flood and drought events (Fig. 5). For instance, extreme wet-to-dry transitions can amplify wildfire risk by allowing increased rates of plant growth and ecosystem biomass accumulation to be immediately followed by rapid drying of flammable vegetation, increasing the potential intensity of subsequent fire events via increased fuel loading<sup>21</sup>, especially in non-forested landscapes<sup>132</sup>. Extreme dry-to-wet transitions, in contrast, can result in increased risk of hydrological hazards (including flash floods and debris flows<sup>133,134</sup>) owing to increased run-off intensity caused by elevated hydrophobicity of soils and/or modification of vegetated land cover resulting from antecedent drought stress<sup>135</sup> or wildfires<sup>136,137</sup>.

Thus, increasingly rapid and large transitions between extreme wet and dry states are likely to challenge not only water and flood management infrastructure<sup>5,138–140</sup>, but also disaster management<sup>141</sup>, emergency response<sup>134</sup> and public health systems<sup>142</sup> that are designed for twentieth-century extremes. Indeed, increases in hydroclimate volatility have the potential to adversely affect climate adaptation efforts. If, for instance, a governmental entity were to predicate future water and flood management primarily upon projected trends in annual mean precipitation in a region such as California — where such trends are projected to be small and/or uncertain in sign<sup>143</sup> — there might be considerable risk of choosing policies and designing infrastructure that would ultimately prove to be inadequate<sup>144</sup> to cope with large projected increases in drought, flood and hydroclimate whiplash events<sup>13,14,92</sup>. Similarly, the tendency for the most extreme but least frequently observed precipitation and subsequent flood events to increase at a faster rate than smaller but more commonly observed events might skew public perceptions in a manner inconsistent with actual shifts in natural hazard risk<sup>113</sup>. Not accounting for such volatility raises the

possibility of costly climate maladaptations, whereby individuals, governments and societies focus too narrowly on a single hazard (droughts at the expense of floods, for instance) and/or are unprepared for the potential impacts of compounding extremes<sup>145</sup>.

### Managing risks of increasing hydroclimate volatility

Given the observed and potential future impacts from hydroclimate volatility, adaptation and mitigation efforts are necessary as existing infrastructure and resource management systems could increasingly be pushed beyond design limits<sup>5</sup>. Successful adaptation will probably require a variety of approaches to co-manage the risks of flood and drought — a large departure from historical norms wherein water overabundance and scarcity were most often managed as separate hazards. Maintaining excessively high reservoir water levels to mitigate drought risk, for instance, could amplify flood risk by rendering the dam structure more vulnerable to overtopping and potential structural damage during subsequent heavy inflows<sup>141</sup>. Conversely, aggressive channelization of rivers for flood control purposes can inhibit groundwater recharge in natural floodplains that might be used as a water source during subsequent droughts<sup>141</sup>.

A number of interventions capable of accommodating increased hydroclimate volatility have, therefore, been proposed and, in some cases, implemented. A common theme across such interventions is flexibility — systems must be able to accommodate a wide range of rapidly changing hydroclimate and hydrological states without compromising their ability to function effectively. One example is floodplain expansion and reconnection, which allows floodwater to spread over a wider area, reducing risks to population centres and critical infrastructure<sup>146</sup>. This nature-based adaptation has the additional potential benefits of mitigating future drought risk and improving water system sustainability via enhanced groundwater recharge, as well as improving riverine and wetland habitats<sup>147</sup>. More technology-intensive interventions include forecast-informed reservoir operations (in which dams are operated in close consultation with meteorologists to use short-term weather forecasts to maximize

water storage without increasing subsequent flood risk<sup>148</sup>), as well as the development of sponge cities designed to decrease the fraction of impervious surfaces to increase infiltration of precipitation into the soil column, yielding the dual benefits of decreased pluvial flood risk and increased aquifer recharge<sup>149</sup>.

## Summary and future perspectives

When antecedent land-surface and hydrological conditions are otherwise favourable, sharp swings between extremely dry and wet hydroclimatic conditions often give rise to disruptively sudden transitions between drought and flood. Such hydroclimate volatility is already observed to have increased globally, especially at subseasonal timescales, and at a rate faster than projected by coarse-resolution climate models (although specific regional trends are less clear historically owing to observational uncertainty). Hydroclimatic volatility is anticipated to further increase in magnitude (by -130% and -50% over land areas, respectively, for subseasonal and interannual whiplash at 3 °C warming above pre-industrial temperature), and to emerge robustly in additional regions as a consequence of anthropogenic climate change. The largest increases are projected to occur across the Northern Hemisphere high latitudes, the Pacific and Atlantic tropical oceans, and in a broad swath extending eastward from northern Africa, across the Arabian Peninsula and into portions of South Asia. Such increases arise primarily from well-understood thermodynamic properties of a warming atmosphere, which dictate an exponential rise in the water-vapour-holding capacity that raises the ceiling on both extreme precipitation and extreme evapotranspiration. There is also potential for additional contributions from changes in the atmospheric circulation, although these are regionally variable and more uncertain. Yet despite confidence that hydroclimate volatility has increased – across a variety of metrics – there remain many limitations or gaps in understanding.

The lack of a uniform definition of hydroclimate volatility is one such challenge. So far, ad hoc, application-specific definitions have been used to capture the magnitude, rate of change and/or frequency of transitions between wet and dry states, with some considering precipitation and others encompassing precipitation and evaporative demand. In envisioning a globally generalizable unifying metric, the SPEI was selected here as the underlying variable for hydroclimate whiplash owing to its ability to capture dry and wet extremes, to capture both precipitation and evaporative demand, and to characterize hydroclimate volatility at the timescales that are most broadly relevant to societal and ecological hazards. However, this metric still has limitations that future metrics could address, namely consideration of: additional characteristics, such as severity, duration, seasonality or affected area; the ‘flavours’ of whiplash, such as precipitation dominated versus evaporative demand dominated, or hydroclimatic versus hydrologic; the inherent spatiotemporal asymmetry between extreme wet and dry events, as well as the possibility that the spatiotemporal dependence between them can itself change; and extremes derived more directly from hydrological and land-surface variables such as run-off and soil moisture.

The offset between the magnitude of observed and modelled trends also highlights a key issue of concern. Notably, observed historical increases in global-scale hydroclimate whiplash are near or above the upper end of projected conditions from the 100-member CESM2-LE (Fig. 2a,c). The possible explanations for this difference highlight several distinct future research directions. First, it is possible that the Earth experienced an ‘unlikely’ iteration of natural variability during the observational period<sup>150</sup>, either related to ENSO or some other internal

mode of variability<sup>75</sup>, temporarily accelerating anthropogenically forced whiplash trends; ongoing efforts to improve understanding of the global sea surface temperature pattern effect<sup>150</sup> and reduce biases in tropical Pacific sea surface temperature gradients<sup>151</sup>, especially through the use of high-resolution (mesoscale eddy-resolving) ocean and/or atmospheric models<sup>152</sup>, might offer a clearer picture. Second, to disentangle observational uncertainty surrounding precipitation extremes and atmospheric evaporative demand from true divergence from predictions, efforts to expand historically sparse and/or discontinuous observational networks<sup>153,154</sup> and improve data assimilation and/or modelling frameworks used in global atmospheric reanalyses<sup>155</sup> will be required. Third, existing Earth system models might directly underestimate the anthropogenically forced rate of change in the wet and dry extremes that underpin hydroclimate volatility; improved representation of very high-intensity, short-duration precipitation extremes<sup>156</sup> using high-resolution<sup>102</sup> (especially convection-resolving<sup>156</sup>) atmospheric models, and of the Earth system processes (including plant water

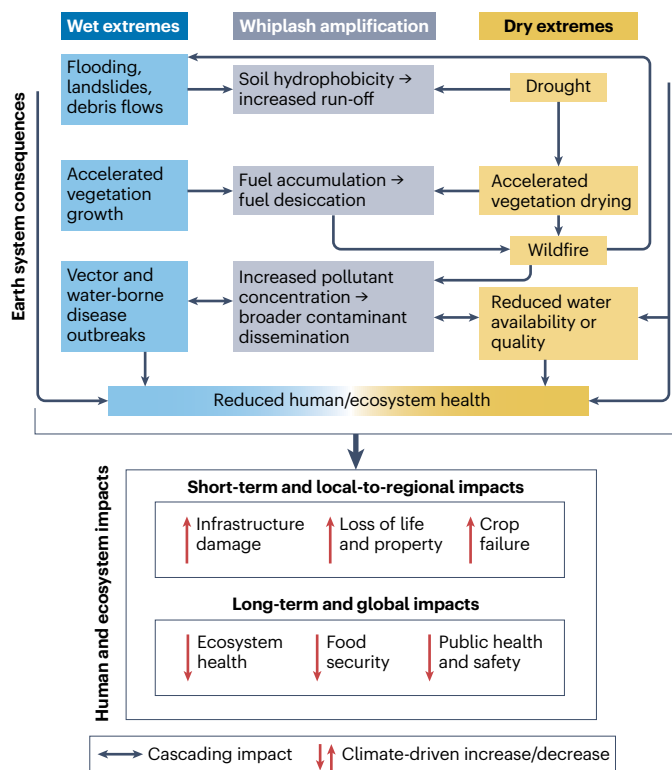


**Fig. 5 | Cascading hydroclimate whiplash hazards in a warming climate.**

The pathways through which hydrological extremes and rapid whiplash transitions between wet and dry states can lead to complex effects in the broader Earth system. The dark arrows represent cascading relationships (in which the initial event causes indirect but substantial downstream effects via an intermediate step or process), and the red vertical arrows show increases or decreases in specific impacts under anthropogenic warming. The processes labelled in blue represent effects caused by wet events alone, those labelled in yellow represent those caused by dry events alone and processes labelled in grey represent those specifically caused by rapid whiplash transitions. Together, natural variability and anthropogenic climate change contribute to meteorological extremes that can cause hydroclimate whiplash events – with subsequent cascading and wide-ranging impacts that are often distinct from wet or dry extremes occurring in isolation.



use, soil moisture and evapotranspiration<sup>157</sup>) related to decreasing specific and RH over continents<sup>158</sup> will also be critical.

Moreover, despite high confidence in the sign of future trends in global-scale hydroclimate whiplash, substantial uncertainties remain with respect to their magnitude and spatial pattern. These uncertainties arise from broader uncertainties surrounding changes to mean and extreme states of atmospheric circulation, including the persistence of atmospheric Rossby waves<sup>159,160</sup> capable of producing long-duration precipitation and temperature extremes<sup>161</sup>, accelerated land-surface feedbacks during extreme heatwaves<sup>162–165</sup>, emergent tipping points in the vegetated biosphere<sup>166–168</sup> and non-stationarity in ENSO and its global hydroclimate teleconnections<sup>80,82,169</sup>. Uncertainty surrounding ENSO, in particular, is the subject of intensifying debate as observed multidecadal trends increasingly conflict with climate model projections<sup>74,75</sup>, raising the question of whether projected trends in regional hydroclimate are realistic and/or whether future forced trends might be non-monotonic<sup>151</sup>.

Future research across many sectors of climate and Earth system science will contribute to resolving these uncertainties. At a large scale, constraining overall global trends in volatility requires narrowing the plausible range of future anthropogenic emission trajectories<sup>170</sup> and associated planetary warming<sup>171</sup>. At a regional scale, understanding the patterns and magnitudes of volatility trends will require methodological advances to examine changes in atmosphere–ocean variability, atmospheric circulation (including those caused by evolving aerosol forcings<sup>172,173</sup>), extreme local storm and subsequent precipitation events<sup>103,156,174</sup>, and feedbacks in the coupled land–biosphere–atmosphere system. These advances could be achieved through both traditional physics-based modelling and emerging machine learning-based methods<sup>175–177</sup>. For the latter, although the near-term prospects for improving multidecadal climate projections and extreme event prediction are potentially transformational<sup>178</sup>, they remain highly uncertain<sup>179</sup>. In addition, measurements of atmospheric and land-surface variables relevant to hydroclimate volatility can be improved through new remote sensing efforts (for example, the NASA SWOT mission)<sup>180</sup>, by increasing the resolution and coverage of historical observations through advanced statistical and machine learning interpolation methods<sup>181</sup>, and by reducing uncertainties in reanalysis products. Additional efforts to couple climate models with hydraulic, dynamic vegetation and/or epidemiological models will offer further insight into the relationship between hydroclimate volatility and its potential impacts, including hydrological drought-to-flood transitions, wildfire risk and disease outbreaks. These efforts will require interdisciplinary collaboration across domains ranging from civil engineering to urban policy and planning to public health, some of which are already underway<sup>182,183</sup>.

Large-ensemble climate modelling experiments are vital for quantifying anthropogenically forced trends in complex atmospheric phenomena that drive hydroclimate volatility. Owing to the relative rarity of such events in historical observations and individual climate model realizations, detecting meaningful and statistically robust trends in the context of annual-to-decadal climate variability can be challenging<sup>42</sup>. Large ensembles of at least several dozens of members run for multiple decades of model-years are often necessary to robustly quantify the probability of statistically rare events<sup>17</sup>, even in the context of strong external forcing. Expanding existing single-model initial condition ensembles to encompass additional dimensions of uncertainty – including parameterizations related to clouds, precipitation and land–atmosphere coupling, as well as a wider range of global and regional anthropogenic and natural climate forcing scenarios<sup>184</sup> – will improve understanding of global

hydroclimate volatility. Likewise, generating large ensembles with sufficiently granular spatial resolution to adequately represent phenomena such as convective precipitation and persistent (blocking) high-pressure systems remains a notable frontier partly owing to computational constraints<sup>185</sup>, but might yield large advances in understanding and predicting volatility-relevant extreme events<sup>156,174</sup>. The need for large ensemble frameworks also extends to observational datasets<sup>186</sup> owing to both persistent spatiotemporal inhomogeneities in observation-sparse regions<sup>187</sup> and differences in representation in the precipitation and evapotranspiration-related processes underpinning whiplash events that can yield notable differences between datasets (Fig. 2 and Supplementary Fig. 1).

Finally, as increases in hydroclimate volatility will have important and widespread consequences, there is an urgent need for disaster management, emergency preparedness, and infrastructure design and operations to incorporate the intensifying risks of compound and cascading impacts. Doing so is necessary to better respond to acute emergencies and to effectively allocate finite climate adaptation resources. This urgency is especially great in central and northern Africa, the Middle East and South Asia given the triple confluence of large projected increases in whiplash (Fig. 3), very high population exposure and underlying socioeconomic factors that increase vulnerability in these regions. Improved understanding of the character, causes and consequences of hydroclimate volatility is thus integral to efforts aimed at managing and reducing the risks of intensifying climate change impacts on a warming Earth.

## Data availability

All ERA5 data are publicly available via <https://cds.climate.copernicus.eu>. NCD20C data are available via <https://rda.ucar.edu/datasets/d131003/dataaccess>. All CESM2-LE data are available via <https://www.cesm.ucar.edu/community-projects/lens2/data-sets>. Hydroclimate whiplash data can be found via the Zenodo repository at <https://doi.org/10.5281/zenodo.13381749> (ref. 188).

## Code availability

Code used to generate hydroclimate whiplash data can be found via the Zenodo repository at <https://doi.org/10.5281/zenodo.13381749> (ref. 188).

Published online: 9 January 2025

## References

1. Ficklin, D. L., Abatzoglou, J. T. & Novick, K. A. A new perspective on terrestrial hydrologic intensity that incorporates atmospheric water demand. *Geophys. Res. Lett.* **46**, 8114–8124 (2019).
2. Giorgi, F. et al. Higher hydroclimatic intensity with global warming. *J. Clim.* **24**, 5309–5324 (2011).
3. Giorgi, F., Raffaele, F. & Coppola, E. The response of precipitation characteristics to global warming from climate projections. *Earth Syst. Dynam.* **10**, 73–89 (2019).
4. Zamora-Reyes, D. et al. The unprecedented character of California's 20th century enhanced hydroclimatic variability in a 600-year context. *Geophys. Res. Lett.* <https://doi.org/10.1029/2022GL099582> (2022).
5. Ficklin, D. L., Null, S. E., Abatzoglou, J. T., Novick, K. A. & Myers, D. T. Hydrological intensification will increase the complexity of water resource management. *Earths Future* <https://doi.org/10.1029/2021EF002487> (2022).
6. Madakumbura, G. D. et al. Event-to-event intensification of the hydrologic cycle from 1.5 °C to a 2 °C warmer world. *Sci. Rep.* **9**, 3483 (2019).
7. Chen, H. & Wang, S. Accelerated transition between dry and wet periods in a warming climate. *Geophys. Res. Lett.* **49**, e2022GL099766 (2022).
8. Cheng, L. & Liu, Z. Detectable increase in global land areas susceptible to precipitation reversals under the RCP8.5 scenario. *Earths Future* **10**, e2022EF002948 (2022).
9. Qing, Y., Wang, S., Yang, Z.-L. & Gentile, P. Soil moisture–atmosphere feedbacks have triggered the shifts from drought to pluvial conditions since 1980. *Commun. Earth Environ.* **4**, 254 (2023).



10. Rashid, M. M. & Wahl, T. Hydrologic risk from consecutive dry and wet extremes at the global scale. *Environ. Res. Commun.* **4**, 071001 (2022).
11. Fang, B. & Lu, M. Asia faces a growing threat from intraseasonal compound weather whiplash. *Earths Future* **11**, e2022EF003111 (2023).
12. Rezvani, R., Na, W. & Najafi, M. R. Lagged compound dry and wet spells in northwest North America under 1.5°C–4°C global warming levels. *Atmos. Res.* **290**, 106799 (2023).
13. Swain, D. L., Langenbrunner, B., Neelin, J. D. & Hall, A. Increasing precipitation volatility in twenty-first-century California. *Nat. Clim. Change* **8**, 427–433 (2018).
14. Chen, D., Norris, J., Thackeray, C. & Hall, A. Increasing precipitation whiplash in climate change hotspots. *Environ. Res. Lett.* **17**, 124011 (2022).
15. Tan, X. et al. Increasing global precipitation whiplash due to anthropogenic greenhouse gas emissions. *Nat. Commun.* **14**, 2796 (2023).
16. Pendergrass, A. G., Knutti, R., Lehner, F., Deser, C. & Sanderson, B. M. Precipitation variability increases in a warmer climate. *Sci. Rep.* **7**, 17966 (2017).
17. Wood, R. R., Lehner, F., Pendergrass, A. G. & Schlunegger, S. Changes in precipitation variability across time scales in multiple global climate model large ensembles. *Environ. Res. Lett.* **16**, 084022 (2021).
18. Zhang, W. et al. Increasing precipitation variability on daily-to-multiyear time scales in a warmer world. *Sci. Adv.* **7**, eabf8021 (2021).
19. Kumar, S., Dewes, C. F., Newman, M. & Duan, Y. Robust changes in North America's hydroclimate variability and predictability. *Earths Future* **11**, e2022EF003239 (2023).
20. Francis, J. A., Skific, N. & Zobel, Z. Weather whiplash events in Europe and North Atlantic assessed as continental-scale atmospheric regime shifts. *npj Clim. Atmos. Sci.* **6**, 216 (2023).
21. Homann, J., Oster, J. L., de Wet, C. B., Breitenbach, S. F. M. & Hoffmann, T. Linked fire activity and climate whiplash in California during the early Holocene. *Nat. Commun.* **13**, 7175 (2022).
22. Trenberth, K. E., Dai, A., Rasmussen, R. M. & Parsons, D. B. The changing character of precipitation. *Bull. Am. Meteorol. Soc.* **84**, 1205–1217 (2003).
23. Fischer, E. M. & Knutti, R. Observed heavy precipitation increase confirms theory and early models. *Nat. Clim. Change* **6**, 986–991 (2016).
24. De Luca, P., Messori, G., Wilby, R. L., Mazzoleni, M. & Di Baldassarre, G. Concurrent wet and dry hydrological extremes at the global scale. *Earth Syst. Dynam.* **11**, 251–266 (2020).
25. Lei, N., Gao, L., Liu, S. & Zhou, Z. The spatiotemporal clustering of short-duration rainstorms in Shanghai city using a sub-hourly gauge network. *Earth Space Sci.* **11**, e2023EA003442 (2024).
26. Herrera-Estrada, J. E. & Diffenbaugh, N. S. Landfalling droughts: global tracking of moisture deficits from the oceans onto land. *Water Resour. Res.* **56**, e2019WR026877 (2020).
27. Williams, A. P., Cook, B. I. & Smerdon, J. E. Rapid intensification of the emerging southwestern North American megadrought in 2020–2021. *Nat. Clim. Change* **12**, 232–234 (2022).
28. Garreaud, R. D. et al. The Central Chile mega drought (2010–2018): a climate dynamics perspective. *Int. J. Climatol.* **40**, 421–439 (2020).
29. Vicente-Serrano, S. M., Begueria, S. & López-Moreno, J. I. A multiscale drought index sensitive to global warming: the standardized precipitation evapotranspiration index. *J. Clim.* **23**, 1696–1718 (2010).
30. Cook, B. I. et al. Twenty-first century drought projections in the CMIP6 forcing scenarios. *Earths Future* **8**, e2019EF001461 (2020).
31. Qing, Y. et al. Accelerated soil drying linked to increasing evaporative demand in wet regions. *npj Clim. Atmos. Sci.* **6**, 205 (2023).
32. Satoh, Y. et al. A quantitative evaluation of the issue of drought definition: a source of disagreement in future drought assessments. *Environ. Res. Lett.* **16**, 104001 (2021).
33. Lintner, B. R. et al. Amplification of wet and dry month occurrence over tropical land regions in response to global warming. *J. Geophys. Res. Atmos.* <https://doi.org/10.1029/2012JD017499> (2012).
34. Albano, C. M. et al. A multidataset assessment of climatic drivers and uncertainties of recent trends in evaporative demand across the continental United States. *J. Hydrometeorol.* **23**, 505–519 (2022).
35. McEvoy, D. J., Pierce, D. W., Kalansky, J. F., Cayan, D. R. & Abatzoglou, J. T. Projected changes in reference evapotranspiration in California and Nevada: implications for drought and wildland fire danger. *Earths Future* **8**, e2020EF001736 (2020).
36. Lloyd-Hughes, B. The impracticality of a universal drought definition. *Theor. Appl. Climatol.* **117**, 607–611 (2014).
37. Van Loon, A. F. et al. Drought in a human-modified world: reframing drought definitions, understanding, and analysis approaches. *Hydrol. Earth Syst. Sci.* **20**, 3631–3650 (2016).
38. Mukherjee, S., Mishra, A. & Trenberth, K. E. Climate change and drought: a perspective on drought indices. *Curr. Clim. Change Rep.* **4**, 145–163 (2018).
39. Hersbach, H. et al. The ERA5 global reanalysis. *Q. J. R. Meteorol. Soc.* **146**, 1999–2049 (2020).
40. Stivinski, L. C. et al. Towards a more reliable historical reanalysis: improvements for version 3 of the Twentieth Century Reanalysis system. *Q. J. R. Meteorol. Soc.* **145**, 2876–2908 (2019).
41. Rodgers, K. B. et al. Ubiquity of human-induced changes in climate variability. *Earth Syst. Dynam.* **12**, 1393–1411 (2021).
42. Deser, C. et al. Insights from Earth system model initial-condition large ensembles and future prospects. *Nat. Clim. Change* **10**, 277–286 (2020).
43. Zhang, W., Zhou, T. & Wu, P. Anthropogenic amplification of precipitation variability over the past century. *Science* **385**, 427–432 (2024).
44. Rodell, M. & Li, B. Changing intensity of hydroclimatic extreme events revealed by GRACE and GRACE-FO. *Nat. Water* <https://doi.org/10.1038/s44221-023-00040-5> (2023).
45. Trenberth, K. E. Conceptual framework for changes of extremes of the hydrological cycle with climate change. *Clim. Change* **42**, 327–339 (1999).
46. Singh, J. et al. Enhanced risk of concurrent regional droughts with increased ENSO variability and warming. *Nat. Clim. Change* **12**, 163–170 (2022).
47. Berg, N. & Hall, A. Increased interannual precipitation extremes over California under climate change. *J. Clim.* **28**, 6324–6334 (2015).
48. Scheff, J. & Frierson, D. M. W. Robust future precipitation declines in CMIP5 largely reflect the poleward expansion of model subtropical dry zones. *Geophys. Res. Lett.* <https://doi.org/10.1029/2012GL052910> (2012).
49. Pfahl, S., O'Gorman, P. A. & Fischer, E. M. Understanding the regional pattern of projected future changes in extreme precipitation. *Nat. Clim. Change* **7**, 423–427 (2017).
50. *IPCC Climate Change 2021: The Physical Science Basis* 1513–1766 (Cambridge Univ. Press, 2023).
51. Hermann, M., Wernli, H. & Röthlisberger, M. Drastic increase in the magnitude of very rare summer-mean vapor pressure deficit extremes. *Nat. Commun.* **15**, 7022 (2024).
52. Li, S. et al. Increasing vapor pressure deficit accelerates land drying. *J. Hydrol.* **625**, 130062 (2023).
53. Novick, K. A. et al. The impacts of rising vapor pressure deficit in natural and managed ecosystems. *Plant Cell Environ.* <https://doi.org/10.1111/pce.14846> (2024).
54. Clapeyron, B.-P. E. Memoir sur la puissance motrice de la chaleur. *J. Éc. Polytech.* **14**, 153–190 (1834).
55. Clausius, R. Ueber die bewegende Kraft der Wärme und die Gesetze, welche sich daraus für die Wärmelehre selbst ableiten lassen. *Annalen der Phys.* **155**, 368–397 (1850).
56. Allan, R. P., Willett, K. M., John, V. O. & Trent, T. Global changes in water vapor 1979–2020. *J. Geophys. Res. Atmos.* **127**, e2022JD036728 (2022).
57. Santer, B. D. et al. Identification of human-induced changes in atmospheric moisture content. *Proc. Natl Acad. Sci. USA* **104**, 15248–15253 (2007).
58. Held, I. M. & Soden, B. J. Robust responses of the hydrological cycle to global warming. *J. Clim.* **19**, 5686–5699 (2006).
59. Emori, S. & Brown, S. J. Dynamic and thermodynamic changes in mean and extreme precipitation under changed climate. *Geophys. Res. Lett.* <https://doi.org/10.1029/2005GL023272> (2005).
60. O'Gorman, P. A. Precipitation extremes under climate change. *Curr. Clim. Change Rep.* **1**, 49–59 (2015).
61. Shaw, T. A. & Voigt, A. Tug of war on summertime circulation between radiative forcing and sea surface warming. *Nat. Geosci.* **8**, 560–566 (2015).
62. Byrne, M. P. & O'Gorman, P. A. Understanding decreases in land relative humidity with global warming: conceptual model and GCM simulations. *J. Clim.* **29**, 9045–9061 (2016).
63. Vicente-Serrano, S. M. et al. Recent changes of relative humidity: regional connections with land and ocean processes. *Earth Syst. Dynam.* **9**, 915–937 (2018).
64. Marvel, K. et al. Twentieth-century hydroclimate changes consistent with human influence. *Nature* **569**, 59–65 (2019).
65. Zhou, W., Leung, L. R. & Lu, J. The role of interactive soil moisture in land drying under anthropogenic warming. *Geophys. Res. Lett.* **50**, e2023GL105308 (2023).
66. Marvel, K. et al. Projected changes to hydroclimate seasonality in the continental United States. *Earths Future* **9**, e2021EF002019 (2021).
67. Breshears, D. et al. The critical amplifying role of increasing atmospheric moisture demand on tree mortality and associated regional die-off. *Front. Plant Sci.* <https://doi.org/10.3389/fpls.2013.00266> (2013).
68. Yuan, W. et al. Increased atmospheric vapor pressure deficit reduces global vegetation growth. *Sci. Adv.* **5**, eaax1396 (2019).
69. Gamelin, B. L. et al. Projected US drought extremes through the twenty-first century with vapor pressure deficit. *Sci. Rep.* **12**, 8615 (2022).
70. Zhuang, Y., Fu, R., Santer, B. D., Dickinson, R. E. & Hall, A. Quantifying contributions of natural variability and anthropogenic forcings on increased fire weather risk over the western United States. *Proc. Natl Acad. Sci. USA* **118**, e2111875118 (2021).
71. Juang, C. S. et al. Rapid growth of large forest fires drives the exponential response of annual forest-fire area to aridity in the western United States. *Geophys. Res. Lett.* **49**, e2021GL097131 (2022).
72. Rao, K., Williams, A. P., Diffenbaugh, N. S., Yebra, M. & Konings, A. G. Plant-water sensitivity regulates wildfire vulnerability. *Nat. Ecol. Evol.* <https://doi.org/10.1038/s41559-021-01654-2> (2022).
73. Yuan, X. et al. A global transition to flash droughts under climate change. *Science* **380**, 187–191 (2023).
74. Lee, S. et al. On the future zonal contrasts of equatorial Pacific climate: perspectives from observations, simulations, and theories. *npj Clim. Atmos. Sci.* **5**, 82 (2022).
75. Seager, R., Henderson, N. & Cane, M. Persistent discrepancies between observed and modeled trends in the tropical Pacific Ocean. *J. Clim.* **35**, 4571–4584 (2022).
76. Neelin, J. D. et al. Precipitation extremes and water vapor. *Curr. Clim. Change Rep.* <https://doi.org/10.1007/s40641-021-00177-z> (2022).
77. *IPCC Climate Change 2021: The Physical Science Basis*, 1055–1210 (Cambridge Univ. Press, 2023).
78. Patricola, C. M. et al. Maximizing ENSO as a source of western US hydroclimate predictability. *Clim. Dyn.* **54**, 351–372 (2020).
79. Alexander, M. A. et al. The atmospheric bridge: the influence of ENSO teleconnections on air–sea interaction over the global oceans. *J. Clim.* **15**, 2205–2231 (2002).
80. Cai, W. et al. Anthropogenic impacts on twentieth-century ENSO variability changes. *Nat. Rev. Earth Environ.* **4**, 407–418 (2023).

81. Zhou, W., Yang, D., Xie, S.-P. & Ma, J. Amplified Madden–Julian oscillation impacts in the Pacific–North America region. *Nat. Clim. Change* **10**, 654–660 (2020).
82. Cai, W. et al. Changing El Niño–Southern Oscillation in a warming climate. *Nat. Rev. Earth Environ.* **2**, 628–644 (2021).
83. Wang, J., Kim, H. & DeFlorio, M. J. Future changes of PNA-like MJO teleconnections in CMIP6 models: underlying mechanisms and uncertainty. *J. Clim.* **35**, 3459–3478 (2022).
84. Chen, G. Diversity of the global teleconnections associated with the Madden–Julian Oscillation. *J. Clim.* **34**, 397–414 (2021).
85. Jenney, A. M., Randall, D. A. & Barnes, E. A. Drivers of uncertainty in future projections of Madden–Julian Oscillation teleconnections. *Weather. Clim. Dyn.* **2**, 653–673 (2021).
86. Shepherd, T. G. Atmospheric circulation as a source of uncertainty in climate change projections. *Nat. Geosci.* **7**, 703–708 (2014).
87. Donat, M. G., Lowry, A. L., Alexander, L. V., Ogorman, P. A. & Maher, N. More extreme precipitation in the world’s dry and wet regions. *Nat. Clim. Change* **6**, 508–513 (2016).
88. Kirchmeier-Young, M. C. & Zhang, X. Human influence has intensified extreme precipitation in North America. *Proc. Natl Acad. Sci. USA* **117**, 13308 (2020).
89. Pendergrass, A. G. et al. Nonlinear response of extreme precipitation to warming in CESM1. *Geophys. Res. Lett.* **46**, 10551–10560 (2019).
90. Swain, D. L. et al. Increased flood exposure due to climate change and population growth in the United States. *Earths Future* **8**, e2020EF001778 (2020).
91. Gründemann, G. J., van de Giesen, N., Brunner, L. & van der Ent, R. Rarest rainfall events will see the greatest relative increase in magnitude under future climate change. *Commun. Earth Environ.* **3**, 235 (2022).
92. Mallakpour, I., Sadegh, M. & AghaKouchak, A. A new normal for streamflow in California in a warming climate: wetter wet seasons and drier dry seasons. *J. Hydrol.* **567**, 203–211 (2018).
93. Chou, C., Neelin, J. D., Chen, C.-A. & Tu, J.-Y. Evaluating the ‘rich-get-richer’ mechanism in tropical precipitation change under global warming. *J. Clim.* **22**, 1982–2005 (2009).
94. Thackeray, C. W., DeAngelis, A. M., Hall, A., Swain, D. L. & Qu, X. On the connection between global hydrologic sensitivity and regional wet extremes. *Geophys. Res. Lett.* **45**, 11,343–11,351 (2018).
95. O’Gorman, P. A. & Muller, C. J. How closely do changes in surface and column water vapor follow Clausius–Clapeyron scaling in climate change simulations? *Environ. Res. Lett.* **5**, 025207 (2010).
96. Martínez-Villalobos, C. & Neelin, J. D. Regionally high risk increase for precipitation extreme events under global warming. *Sci. Rep.* **13**, 5579 (2023).
97. Kotz, M., Lange, S., Wenz, L. & Levermann, A. Constraining the pattern and magnitude of projected extreme precipitation change in a multimodel ensemble. *J. Clim.* **37**, 97–111 (2024).
98. Pendergrass, A. G. & Hartmann, D. L. The atmospheric energy constraint on global-mean precipitation change. *J. Clim.* **27**, 757–768 (2014).
99. Gu, G. & Adler, R. F. Precipitation intensity changes in the tropics from observations and models. *J. Clim.* **31**, 4775–4790 (2018).
100. Polade, S. D., Pierce, D. W., Cayan, D. R., Gershunov, A. & Dettinger, M. D. The key role of dry days in changing regional climate and precipitation regimes. *Sci. Rep.* **4**, 4364 (2014).
101. Wainwright, C. M., Black, E. & Allan, R. P. Future changes in wet and dry season characteristics in CMIP5 and CMIP6 simulations. *J. Hydrometeorol.* **22**, 2339–2357 (2021).
102. Lenderink, G. et al. Scaling and responses of extreme hourly precipitation in three climate experiments with a convection-permitting model. *Philos. Trans. R. Soc. A* **379**, 20190544 (2021).
103. Lenderink, G., Barbero, R., Loriaux, J. M. & Fowler, H. J. Super-Clausius–Clapeyron scaling of extreme hourly convective precipitation and its relation to large-scale atmospheric conditions. *J. Clim.* **30**, 6037–6052 (2017).
104. Pendergrass, A. G. What precipitation is extreme? *Science* **360**, 1072 (2018).
105. Fowler, H. J. et al. Anthropogenic intensification of short-duration rainfall extremes. *Nat. Rev. Earth Environ.* **2**, 107–122 (2021).
106. Liu, M., Vecchi, G. A., Smith, J. A. & Knutson, T. R. Causes of large projected increases in hurricane precipitation rates with global warming. *npj Clim. Atmos. Sci.* **2**, 38 (2019).
107. Prein, A. F. et al. Increased rainfall volume from future convective storms in the US. *Nat. Clim. Change* **7**, 880–884 (2017).
108. Berghuis, W. R., Harrigan, S., Molnar, P., Slater, L. J. & Kirchner, J. W. The relative importance of different flood-generating mechanisms across Europe. *Water Resour. Res.* **55**, 4582–4593 (2019).
109. Brunner, M. I. et al. An extremeness threshold determines the regional response of floods to changes in rainfall extremes. *Commun. Earth Environ.* **2**, 173 (2021).
110. Davenport, F. V., Herrera-Estrada, J. E., Burke, M. & Duffenbaugh, N. S. Flood size increases nonlinearly across the western United States in response to lower snow-precipitation ratios. *Water Resour. Res.* **56**, e2019WR025571 (2020).
111. Gu, X. et al. Attribution of global soil moisture drying to human activities: a quantitative viewpoint. *Geophys. Res. Lett.* <https://doi.org/10.1029/2018GL080768> (2019).
112. Wilhelm, B. et al. Impact of warmer climate periods on flood hazard in the European Alps. *Nat. Geosci.* **15**, 118–123 (2022).
113. Wasko, C., Guo, D., Ho, M., Nathan, R. & Vogel, E. Diverging projections for flood and rainfall frequency curves. *J. Hydrol.* **620**, 129403 (2023).
114. Quintero, F., Villarini, G., Prein, A. F., Zhang, W. & Krajewski, W. F. Discharge and floods projected to increase more than precipitation extremes. *Hydrol. Process.* **36**, e14738 (2022).
115. Feng, L. et al. Harmful algal blooms in inland waters. *Nat. Rev. Earth Environ.* **5**, 631–644 (2024).
116. Loecke, T. D. et al. Weather whiplash in agricultural regions drives deterioration of water quality. *Biogeochemistry* **133**, 7–15 (2017).
117. Paul, M. J. et al. Wildfire induces changes in receiving waters: a review with considerations for water quality management. *Water Resour. Res.* **58**, e2021WR030699 (2022).
118. Zhu, R. et al. Cumulative effects of drought–flood abrupt alternation on the photosynthetic characteristics of rice. *Environ. Exp. Bot.* **169**, 103901 (2020).
119. Chen, H. & Wang, S. Compound dry and wet extremes lead to an increased risk of rice yield loss. *Geophys. Res. Lett.* **50**, e2023GL105817 (2023).
120. Vadez, V. et al. Crop traits and production under drought. *Nat. Rev. Earth Environ.* **5**, 211–225 (2024).
121. Matano, A., de Ruiter, M. C., Koehler, J., Ward, P. J. & Van Loon, A. F. Caught between extremes: understanding human–water interactions during drought-to-flood events in the Horn of Africa. *Earths Future* **10**, e2022EF002747 (2022).
122. Sloat, L. L. et al. Increasing importance of precipitation variability on global livestock grazing lands. *Nat. Clim. Change* **8**, 214–218 (2018).
123. Reed, C. et al. The impact of flooding on food security across Africa. *Proc. Natl Acad. Sci. USA* **119**, e2119399119 (2022).
124. Liu, X., Zhang, D. & He, X. Unveiling the role of climate in spatially synchronized locust outbreak risks. *Sci. Adv.* **10**, ead1164 (2024).
125. Gage, K. L., Burkot, T. R., Eisen, R. J. & Hayes, E. B. Climate and vectorborne diseases. *Am. J. Prev. Med.* **35**, 436–450 (2008).
126. Caminade, C., McIntyre, K. M. & Jones, A. E. Impact of recent and future climate change on vector-borne diseases. *Ann. N. Y. Acad. Sci.* **1436**, 157–173 (2019).
127. Rieckmann, A., Tamason, C. C., Gurlley, E. S., Rod, N. H. & Jensen, P. K. M. Exploring droughts and floods and their association with cholera outbreaks in sub-Saharan Africa: a register-based ecological study from 1990 to 2010. *Am. J. Trop. Med. Hyg.* **98**, 1269–1274 (2018).
128. Head, J. R. et al. Effects of precipitation, heat, and drought on incidence and expansion of coccidioidomycosis in western USA: a longitudinal surveillance study. *Lancet Planet. Health* **6**, e793–e803 (2022).
129. Tichavský, R., Ballesteros-Cánovas, J. A., Šilhán, K., Tolasz, R. & Stoffel, M. Dry spells and extreme precipitation are the main trigger of landslides in Central Europe. *Sci. Rep.* **9**, 14560 (2019).
130. Vahedifard, F., Williams, J. & AghaKouchak, A. Geotechnical engineering in the face of climate change: role of multi-physics processes in partially saturated soils. In *International Foundation Congress and Equipment Expo 2018* (American Society of Civil Engineers, 2018); <https://doi.org/10.1061/9780784481585.035>.
131. Robinson, J. D. & Vahedifard, F. Weakening mechanisms imposed on California’s levees under multiyear extreme drought. *Clim. Change* **137**, 1–14 (2016).
132. Jones, M. W. et al. Global and regional trends and drivers of fire under climate change. *Rev. Geophys.* **60**, e2020RG000726 (2022).
133. DeGraff, J. V., Cannon, S. H. & Gartner, J. E. The timing of susceptibility to post-fire debris flows in the western United States. *Environ. Eng. Geosci.* **21**, 277–292 (2015).
134. Oakley, N. S. A warming climate adds complexity to post-fire hydrologic hazard planning. *Earths Future* **9**, e2021EF002149 (2021).
135. Hubbert, K. R., Wohlgemuth, P. M., Beyers, J. L., Narog, M. G. & Gerrard, R. Post-fire soil water repellency, hydrologic response, and sediment yield compared between grass-converted and chaparral watersheds. *Fire Ecol.* **8**, 143–162 (2012).
136. Jacobs, L. et al. Reconstruction of a flash flood event through a multi-hazard approach: focus on the Rwenzori Mountains, Uganda. *Nat. Hazards* **84**, 851–876 (2016).
137. Touma, D. et al. Climate change increases risk of extreme rainfall following wildfire in the western United States. *Sci. Adv.* **8**, eabm0320 (2022).
138. Mallakpour, I., AghaKouchak, A. & Sadegh, M. Climate-induced changes in the risk of hydrological failure of major dams in California. *Geophys. Res. Lett.* <https://doi.org/10.1029/2018GL081888> (2019).
139. Lopez-Cantu, T., Webber, M. K. & Samaras, C. Incorporating uncertainty from downscaled rainfall projections into climate resilience planning in US cities. *Environ. Res. Infrastruct. Sustain.* **2**, 045006 (2022).
140. Schlef, K. E. et al. Review: incorporating non-stationarity from climate change into rainfall frequency and intensity–duration–frequency (IDF) curves. *J. Hydrol.* <https://doi.org/10.1016/j.jhydrol.2022.128757> (2022).
141. Ward, P. J. et al. The need to integrate flood and drought disaster risk reduction strategies. *Water Secur.* **11**, 100070 (2020).
142. Ebi, K. L. et al. Extreme weather and climate change: population health and health system implications. *Annu. Rev. Public Health* **42**, 293–315 (2021).
143. Neelin, J. D., Langenbrunner, B., Meyerson, J. E., Hall, A. & Berg, N. California winter precipitation change under global warming in the coupled model intercomparison project phase 5 ensemble. *J. Clim.* **26**, 6238–6256 (2013).
144. Persad, G. G., Swain, D. L., Kouba, C. & Ortiz-Partida, J. P. Inter-model agreement on projected shifts in California hydroclimate characteristics critical to water management. *Clim. Change* **162**, 1493–1513 (2020).
145. Zscheischler, J. et al. A typology of compound weather and climate events. *Nat. Rev. Earth Environ.* **1**, 333–347 (2020).
146. Opperman, J. et al. Sustainable floodplains through large-scale reconnection to rivers. *Science* **326**, 1487–1488 (2009).
147. He, X. et al. Climate-informed hydrologic modeling and policy typology to guide managed aquifer recharge. *Sci. Adv.* **7**, eabe6025 (2021).
148. Delaney, C. J. et al. Forecast informed reservoir operations using ensemble streamflow predictions for a multipurpose reservoir in Northern California. *Water Resour. Res.* **56**, e2019WR026604 (2020).

149. Chan, F. K. S. et al. ‘Sponge City’ in China — a breakthrough of planning and flood risk management in the urban context. *Land Use Policy* **76**, 772–778 (2018).
150. Armour, K. C. et al. Sea-surface temperature pattern effects have slowed global warming and biased warming-based constraints on climate sensitivity. *Proc. Natl Acad. Sci. USA* **121**, e2312093121 (2024).
151. Maher, N. et al. The future of the El Niño–Southern Oscillation: using large ensembles to illuminate time-varying responses and inter-model differences. *Earth Syst. Dynam.* **14**, 413–431 (2023).
152. Wengel, C. et al. Future high-resolution El Niño/Southern Oscillation dynamics. *Nat. Clim. Change* **11**, 758–765 (2021).
153. Lamptey, B. et al. Challenges and ways forward for sustainable weather and climate services in Africa. *Nat. Commun.* **15**, 2664 (2024).
154. Tzachor, A. et al. How to reduce Africa’s undue exposure to climate risks. *Nature* **620**, 488–491 (2023).
155. Muñoz-Sabater, J. et al. ERA5-Land: a state-of-the-art global reanalysis dataset for land applications. *Earth Syst. Sci. Data* **13**, 4349–4383 (2021).
156. Fossier, G. et al. Convection-permitting climate models offer more certain extreme rainfall projections. *npj Clim. Atmos. Sci.* **7**, 51 (2024).
157. Zhao, M., A. G., Liu, Y. & Konings, A. G. Evapotranspiration frequently increases during droughts. *Nat. Clim. Change* **12**, 1024–1030 (2022).
158. Simpson, I. R. et al. Observed humidity trends in dry regions contradict climate models. *Proc. Natl Acad. Sci. USA* **121**, e2302480120 (2024).
159. Mann, M. E. et al. Projected changes in persistent extreme summer weather events: the role of quasi-resonant amplification. *Sci. Adv.* **4**, eaat3272 (2018).
160. White, R. H., Kornhuber, K., Martius, O. & Wirth, V. From atmospheric waves to heatwaves: a waveguide perspective for understanding and predicting concurrent, persistent, and extreme extratropical weather. *Bull. Am. Meteorol. Soc.* **103**, E923–E935 (2022).
161. Kautz, L. A. et al. Atmospheric blocking and weather extremes over the Euro-Atlantic sector — a review. *Weather Clim. Dyn.* **3**, 305–336 (2022).
162. Qiao, L. et al. Soil moisture–atmosphere coupling accelerates global warming. *Nat. Commun.* **14**, 4908 (2023).
163. Bartusek, S., Kornhuber, K. & Ting, M. 2021 North American heatwave amplified by climate change-driven nonlinear interactions. *Nat. Clim. Change* **12**, 1143–1150 (2022).
164. Wehrli, K., Guillod, B. P., Hauser, M., Leclair, M. & Seneviratne, S. I. Identifying key driving processes of major recent heat waves. *J. Geophys. Res. Atmos.* **124**, 11746–11765 (2019).
165. Miralles, D. G., Teuling, A. J., van Heerwaarden, C. C. & Vilà-Guerau de Arellano, J. Mega-heatwave temperatures due to combined soil desiccation and atmospheric heat accumulation. *Nat. Geosci.* **7**, 345–349 (2014).
166. Flores, B. M. et al. Critical transitions in the Amazon forest system. *Nature* **626**, 555–564 (2024).
167. Allen, C. D., Breshears, D. D. & McDowell, N. G. On underestimation of global vulnerability to tree mortality and forest die-off from hotter drought in the Anthropocene. *Ecosphere* **6**, art129 (2015).
168. Wion, A. P. et al. Dead again: predictions of repeat tree die-off under hotter droughts confirm mortality thresholds for a dryland conifer species. *Environ. Res. Lett.* **17**, 074031 (2022).
169. Haszpra, T., Herein, M. & Bóday, T. Investigating ENSO and its teleconnections under climate change in an ensemble view — a new perspective. *Earth Syst. Dynam.* **11**, 267–280 (2020).
170. *IPCC Climate Change 2021: The Physical Science Basis* 553–672 (Cambridge Univ. Press, 2023).
171. Sherwood, S. C. et al. An assessment of Earth’s climate sensitivity using multiple lines of evidence. *Rev. Geophys.* **58**, e2019RG000678 (2020).
172. Dong, B. & Sutton, R. T. Recent trends in summer atmospheric circulation in the North Atlantic/European region: is there a role for anthropogenic aerosols? *J. Clim.* **34**, 6777–6795 (2021).
173. Wang, Y. et al. Reduced European aerosol emissions suppress winter extremes over northern Eurasia. *Nat. Clim. Change* **10**, 225–230 (2020).
174. Ban, N. et al. The first multi-model ensemble of regional climate simulations at kilometer-scale resolution, part I: evaluation of precipitation. *Clim. Dyn.* **57**, 275–302 (2021).
175. de Burgh-Day, C. O. & Leeuwenburg, T. Machine learning for numerical weather and climate modelling: a review. *Geosci. Model. Dev.* **16**, 6433–6477 (2023).
176. Molina, M. J. et al. A review of recent and emerging machine learning applications for climate variability and weather phenomena. *Artif. Intell. Earth Syst.* **2**, 220086 (2023).
177. Schneider, T., Leung, L. R. & Wills, R. C. J. Opinion: optimizing climate models with process knowledge, resolution, and artificial intelligence. *Atmos. Chem. Phys.* **24**, 7041–7062 (2024).
178. Davenport, F. V., Barnes, E. A. & Gordon, E. M. Combining neural networks and CMIP6 simulations to learn windows of opportunity for skillful prediction of multiyear sea surface temperature variability. *Geophys. Res. Lett.* **51**, e2023GL108099 (2024).
179. Wong, C. How AI is improving climate forecasts. *Nature* <https://doi.org/10.1038/d41586-024-00780-8> (2024).
180. Biancamaria, S., Lettenmaier, D. P. & Pavelsky, T. M. The SWOT mission and its capabilities for land hydrology. *Surv. Geophys.* **37**, 307–337 (2016).
181. Koldunov, N. et al. Emerging AI-based weather prediction models as downscaling tools. Preprint at <https://doi.org/10.48550/arXiv.2406.17977> (2024).
182. Carlson, C. J., Alam, M. S., North, M. A., Onyango, E. & Stewart-Ibarra, A. M. The health burden of climate change: a call for global scientific action. *PLoS Clim.* **2**, e0000126 (2023).
183. Ayyub, B., DeAngelo, B., Walker, D. & Barsugli, J. ASCE–NOAA workshops on leveraging Earth system science and modeling to inform civil engineering design. NOAA <https://doi.org/10.25923/e8kn-n884> (2023).
184. Fyfe, J. C., Kharin, V. V., Santer, B. D., Cole, J. N. S. & Gillett, N. P. Significant impact of forcing uncertainty in a large ensemble of climate model simulations. *Proc. Natl Acad. Sci. USA* **118**, e2016549118 (2021).
185. Kendon, E. J., Prein, A. F., Senior, C. A. & Stirling, A. Challenges and outlook for convection-permitting climate modelling. *Philos. Trans. R. Soc. A* **379**, 20190547 (2021).
186. McKinnon, K. A., Poppick, A., Dunn-Sigouin, E. & Deser, C. An ‘Observational Large Ensemble’ to compare observed and modeled temperature trend uncertainty due to internal variability. *J. Clim.* **30**, 7585–7598 (2017).
187. Tian, T., Yang, S., Høyer, J. L., Nielsen-Englyst, P. & Singha, S. Cooler Arctic surface temperatures simulated by climate models are closer to satellite-based data than the ERA5 reanalysis. *Commun. Earth Environ.* **5**, 111 (2024).
188. Swain, D. L. et al. Zenodo <https://doi.org/10.5281/zenodo.13381749> (2024).
189. Pendergrass, A. G. & Knutti, R. The uneven nature of daily precipitation and its change. *Geophys. Res. Lett.* <https://doi.org/10.1029/2018GL080298> (2018).
190. Myhre, G. et al. Frequency of extreme precipitation increases extensively with event rareness under global warming. *Sci. Rep.* **9**, 16063 (2019).
191. Zeder, J. & Fischer, E. M. Observed extreme precipitation trends and scaling in Central Europe. *Weather Clim. Extrem.* **29**, 100266 (2020).
192. Sun, Q., Zhang, X., Zwiers, F., Westra, S. & Alexander, L. V. A global, continental, and regional analysis of changes in extreme precipitation. *J. Clim.* **34**, 243–258 (2021).
193. Madakumbura, G. D., Thackeray, C. W., Norris, J., Goldenson, N. & Hall, A. Anthropogenic influence on extreme precipitation over global land areas seen in multiple observational datasets. *Nat. Commun.* **12**, 3944 (2021).
194. Slater, L. et al. Global changes in 20-year, 50-year, and 100-year river floods. *Geophys. Res. Lett.* **48**, e2020GL091824 (2021).
195. Bertola, M., Viglione, A., Lun, D., Hall, J. & Blöschl, G. Flood trends in Europe: are changes in small and big floods different? *Hydrol. Earth Syst. Sci.* **24**, 1805–1822 (2020).
196. Blöschl et al. Changing climate both increases and decreases European river floods. *Nature* **573**, 108–111 (2019).
197. Archfield, S. A., Hirsch, R. M., Viglione, A. & Blöschl, G. Fragmented patterns of flood change across the United States. *Geophys. Res. Lett.* **43**, 10,232–210,239 (2016).
198. Sharma, A., Wasko, C. & Lettenmaier, D. P. If precipitation extremes are increasing, why aren’t floods? *Water Resour. Res.* **54**, 8545–8551 (2018).
199. Brunner, M. I. & Slater, L. J. Extreme floods in Europe: going beyond observations using reforecast ensemble pooling. *Hydrol. Earth Syst. Sci.* **26**, 469–482 (2022).
200. Wasko, C., Nathan, R., Stein, L. & O’Shea, D. Evidence of shorter more extreme rainfalls and increased flood variability under climate change. *J. Hydrol.* **603**, 126994 (2021).
201. Wasko, C. & Nathan, R. Influence of changes in rainfall and soil moisture on trends in flooding. *J. Hydrol.* **575**, 432–441 (2019).

## Acknowledgements

D.L.S. was supported through a collaboration between UCLA, the NSF National Science Foundation National Center for Atmospheric Research and The Nature Conservancy of California. M.B. acknowledges funding from the Swiss National Science Foundation SNSF through the ‘Consecutive drought-flood events in a warming world’ project (ConDF, grant number 200021\_214907). This material is based upon work supported by the NSF National Center for Atmospheric Research, which is a major facility sponsored by the US National Science Foundation under Cooperative Agreement No. 1852977.

## Author contributions

Conceptualization by D.L.S., A.F.P., J.T.A., C.M.A., M.B., N.S.D., D.S., C.B.S. and D.T. Methodology by D.L.S., A.F.P., J.T.A., C.M.A., M.B., N.S.D., D.S., C.B.S. and D.T. Data acquisition and curation by D.L.S., A.F.P. and J.T.A. Investigation by D.L.S., A.F.P. and J.T.A. Visualization by D.L.S., A.F.P., J.T.A., D.S. and C.B.S. Writing — original draft by D.L.S. Writing — review and editing by D.L.S., A.F.P., J.T.A., C.M.A., M.B., N.S.D., D.S., C.B.S. and D.T. Project administration by D.L.S.

## Competing interests

The authors declare no competing interests.

## Additional information

**Supplementary information** The online version contains supplementary material available at <https://doi.org/10.1038/s43017-024-00624-z>.

**Peer review information** *Nature Reviews Earth & Environment* thanks Paolo de Luca, Xuezhong Tan, Shuo Wang and the other, anonymous, reviewers for their contribution to the peer review of this work.

**Publisher’s note** Springer Nature remains neutral with regard to jurisdictional claims in published maps and institutional affiliations.

Springer Nature or its licensor (e.g. a society or other partner) holds exclusive rights to this article under a publishing agreement with the author(s) or other rightsholder(s); author self-archiving of the accepted manuscript version of this article is solely governed by the terms of such publishing agreement and applicable law.

© Springer Nature Limited 2025

---

<sup>1</sup>University of California Agriculture and Natural Resources, Davis, CA, USA. <sup>2</sup>Institute of the Environment and Sustainability, University of California, Los Angeles, CA, USA. <sup>3</sup>Capacity Center for Climate and Weather Extremes, National Center for Atmospheric Research (NCAR), Boulder, CO, USA. <sup>4</sup>Institute for Atmospheric and Climate Science, ETH Zürich, Zurich, Switzerland. <sup>5</sup>Management of Complex Systems, University of California, Merced, CA, USA. <sup>6</sup>Division of Hydrologic Sciences, Desert Research Institute, Reno, NV, USA. <sup>7</sup>Department of Environmental Systems Science, ETH Zürich, Zurich, Switzerland. <sup>8</sup>WSL Institute for Snow and Avalanche Research SLF, Davos, Switzerland. <sup>9</sup>Climate Change, Extremes and Natural Hazards in Alpine Regions Research Center CERC, Davos, Switzerland. <sup>10</sup>Doerr School of Sustainability, Stanford University, Stanford, CA, USA. <sup>11</sup>School of the Environment, Washington State University, Vancouver, WA, USA. <sup>12</sup>Department of Environmental Earth and Atmospheric Sciences, University of Massachusetts, Lowell, MA, USA. <sup>13</sup>Institute for Geophysics, University of Texas, Austin, TX, USA.